GSFC 421.7-70-03
Release Date: August 2010
Expiration Date: August 2015
Revision -
Code 426

GLORY PROJECT

Aerosol Polarimetry Sensor Calibration

AEROSOL POLARIMETRY SENSOR

ALGORITHM THEORETIC BASIS DOCUMENT

August 2010
Revision -

GODDARD SPACE FLIGHT CENTER
GREENBELT, MARYLAND

Aerosol Polarimetry Sensor Calibration

AEROSOL POLARIMETRY SENSOR

ALGORITHM THEORETIC BASIS DOCUMENT

Signature Page

PREPARED AND APPROVED BY:

______________________________ ________________

Brian Cairns Date

NASA Goddard Institute for Space Studies

______________________________ ________________

Igor Geogdzhayev Date

Columbia University

DOCUMENT HISTORY LOG

Document Title: Aerosol Polarimetry Sensor Calibration

AEROSOL POLARIMETRY SENSOR ALGORITHM THEORETIC BASIS DOCUMENT

Release Date : August 2010

Status (Baseline/ Revision/ Canceled)	Document Revision	Effective Date	Description
Baseline	Baseline	August 2010	Approved by CCR 426 - TBD

Table of Contents

1. INTRODUCTION 1
1.1. Overview 1
1.2. Purpose 2
1.3. Scope 2
1.4. Documents 2
1.5. Requirements 2
2. CALIBRATION - THEORETICAL BASIS 5
2.1. APS Data 5
2.1.1. APS System Model 6
2.1.2. APS Calibration Coefficients 13
2.1.3. APS Calibration Implementation 13
3. RADIOMETRIC CALIBRATION 15
3.1. Introduction 15
3.2. Discussion 15
3.3. Alternative Methods for Radiometric Calibration of APS 18
3.3.1. Reflectance Based 18
3.3.2. Radiance Based 19
3.4. Summary of Radiometric Calibration Approach 20
3.5. Solar Reference Calibration 20
3.6. Lunar Calibration 21
3.6.1. Lunar Calibration Maneuver 21
3.6.2. Lunar Calibration Correction Factors 22
3.6.2.1. Sun, Moon, Instrument Distances 22
3.6.2.2. Oversampling Correction 22
3.6.2.3. Lunar Phase Angle and Libration Effects 23
4. POLARIMETRIC CALIBRATION 25
4.1. Unpolarized Reference Calibration 25
4.2. Polarized Reference Calibration 27
5. REFERENCES 27

1. INTRODUCTION

In order for the Aerosol Polarimetry Sensor (APS) data to be of use in scientific algorithms that derive geophysical parameters it needs to be calibrated. The APS calibration comprises a combination of pre-launch and on-orbit calibration and characterization procedures, including both radiometry and polarimetry. This Algorithm Theoretic Basis Document (ATBD) describes the planned operational calibration of APS data.

It is a working document in the sense that depending on the nature, scope and performance of the APS sensor the actual algorithms that are implemented may be adjusted compared with those presented in this version of the ATBD. Nonetheless, the system model and approach presented here are complete and any adaptation of the calibration algorithms would be the result of the failure of the APS sensor to meet its performance requirements and a consequent need to include error terms, that are currently expected to be negligible, in the calibration process.

1.1. Overview

APS calibration has two components to it: (i) pre-launch characterization and calibration and (ii) on-orbit calibration.

For APS polarimetry, a critical requirement pre-launch is to characterize the polarization angle orientation of the analyzers to ensure polarimetric accuracy and knowledge of polarimetric azimuth, as well as geometric alignments to ensure instantaneous field of view (IFOV) matching. The absolute spectral response of each APS band must also be measured in order to be able to relate operational measurements, with a solar spectral distribution, to the standard ground-based radiometric calibration using a NIST traceable integrating sphere source that is the basis for the pre-launch radiometric calibration. Polarization precision is primarily dependent on signal to noise ratio (SNR) which will also be measured and characterized prior to launch and which will be tracked on orbit.

To ensure that the polarization characteristics of the APS can be tracked on orbit and that the required high polarimetric accuracy is achieved for the range of actual operating conditions, both unpolarized and polarized references using “earthshine” are incorporated within the APS design so as to provide known polarization inputs over the dynamic range and with spectral content similar to the scenes of interest. The offsets and gains that define the APS radiometric scale are determined from onboard dark and solar references respectively, in conjunction with lunar calibration. The solar reference provides a definition of the reflectance scale at the time that its protective cover is deployed. It will subsequently degrade due to UV curing of the Spectralon reflector, and the long term radiometric stability will therefore be tracked using lunar calibrations at the same phase of the moon each lunar cycle.

1.2. Purpose

This Algorithm Theoretic Basis Document (ATBD) describes the processes required to transform raw (level 0) data into calibrated (level 1) data. Specifically this document defines the calibration coefficients required for APS and their sources and how they are used.

1.3. Scope

This document describes the operational calibration of APS data. Planned measurements pre-launch that provide calibration coefficients are identified but the tests used for their derivation are only described at a high level. The calibrators that are used as the source of calibration coefficients that are generated on-orbit are discussed in more detail and the algorithms used for the generation of those calibration coefficients are described. The planned numerical method for converting APS digital numbers into calibrated (polarized) radiances and reflectances is also described here.

Section 1 describes the purpose and scope of this document and provides an overview of the calibration approach for APS. Section 2 introduces the equations used to convert digital numbers (DN) from the APS into calibrated (polarized) radiances and reflectances and defines the calibration coefficients that are required in order to do this. Section 3 describes the sources for the various calibration coefficients and, for the coefficients that are derived from the on-orbit dark, unpolarized and polarized references, the planned operational method for their derivation. Section 4 describes the operational use of the solar reference and lunar calibration. Section 5 provides references.

1.4. Documents

The reference document for the requirements that the APS calibration algorithm must meet is the *NASA Glory Science and Mission Requirements Document* (SMRD). Should there be a discrepancy between the requirements stated in this document and the SMRD, the SMRD shall take precedence.

The information contained in this document is also dependent on the:

APS Calibration and Characterization Plan
APS Sensor Command and Telemetry Handbook
NASA Glory Flight Operations Handbook

1.5. Requirements

Those requirements from the SMRD (Rev-B) that the APS calibration process must meet are replicated here for ease of reference

1.5.1 *The radiometric accuracy and precision of the APS shall be as described in Table 1.5-1. Polarization accuracy is considered to be the absolute accuracy of the determination of the normalized Stokes parameters q and u for each telescope, with a functional variation with measured value as defined in Figure 1.5-1. The relative spectral accuracy is considered to be the accuracy with which the ratio of the radiances in spectrally adjacent bands can be determined. The plane of reference for q and u polarization* *measurements is the meridional plane defined by the APS scanner. APS radiometric calibration should be traceable to NIST standards. The function e(P) is used to specify polarimetric accuracy as a function of polarization value. e(P) is defined to be: $e(P)=0.002$ when $P<0.2$ and $e(P)=0.002+0.00375(P-0.2)$ when $P>0.2$. The function S(DN) is the intensity expressed in units of digital number after any correction for dark count and non-linearity. Refer to Section 9 for a definition of the S(DN) parameter.*

1.5.2 Radiometric calibration and the accuracy of the APS sensor as determined on-orbit shall be traceable to a reflectance-based scale , since the accuracy requirements for the APS sensor apply particularly to knowledge of the reflectance of the observed earth scenes.

1.5.3 The reflectance based scale shall be established by the APS sensor during the initial deployment. The reflectance based scale will be maintained using lunar calibration for the remainder of the mission.

1.5.4 The APS radiometric accuracy over the entire spectral range shall be stable to within 0.3% per year over the period of performance of three years.

1.5.5 The APS polarimetric accuracy over the entire spectral range shall be stable to within 0.1% per year over the period of performance of three years.

Band	λ (nm)	Radiometric (Reflectance-based)			Polarization	
		Absolute Accuracy (1σ)	Relative Spectral Accuracy (1σ)	Precision (1σ)	Accuracy (1σ)	Precision (1σ)
P1	412	0.05 + 2/S(DN)	0.013+4/S(DN)	0.008	e(P)+2/S(DN)	0.003
P2	443	0.05 + 2/S(DN)	0.013+4/S(DN)	0.008	e(P)+2/S(DN)	0.003
P3	555	0.05 + 2/S(DN)	0.013+4/S(DN)	0.008	e(P)+2/S(DN)	0.003
P4	672	0.05 + 2/S(DN)	0.013+4/S(DN)	0.008	e(P)+2/S(DN)	0.003
P5	865	0.05 + 2/S(DN)	0.013+4/S(DN)	0.008	e(P)+2/S(DN)	0.003
P6	910	0.05 + 2/S(DN)	0.013+4/S(DN)	0.01	e(P)+2/S(DN)	0.0075
P7	1378	0.08 + 2/S(DN)	0.02+4/S(DN)	0.008	e(P)+2/S(DN)	0.005
P8	1610	0.05 + 2/S(DN)	0.02+4/S(DN)	0.008	e(P)+2/S(DN)	0.003
P9	2250	0.05 + 2/S(DN)	0.02+4/S(DN)	0.008	e(P)+2/S(DN)	0.003

Table 1.5-1 APS Radiometric and Polarimetric Accuracy and Precision

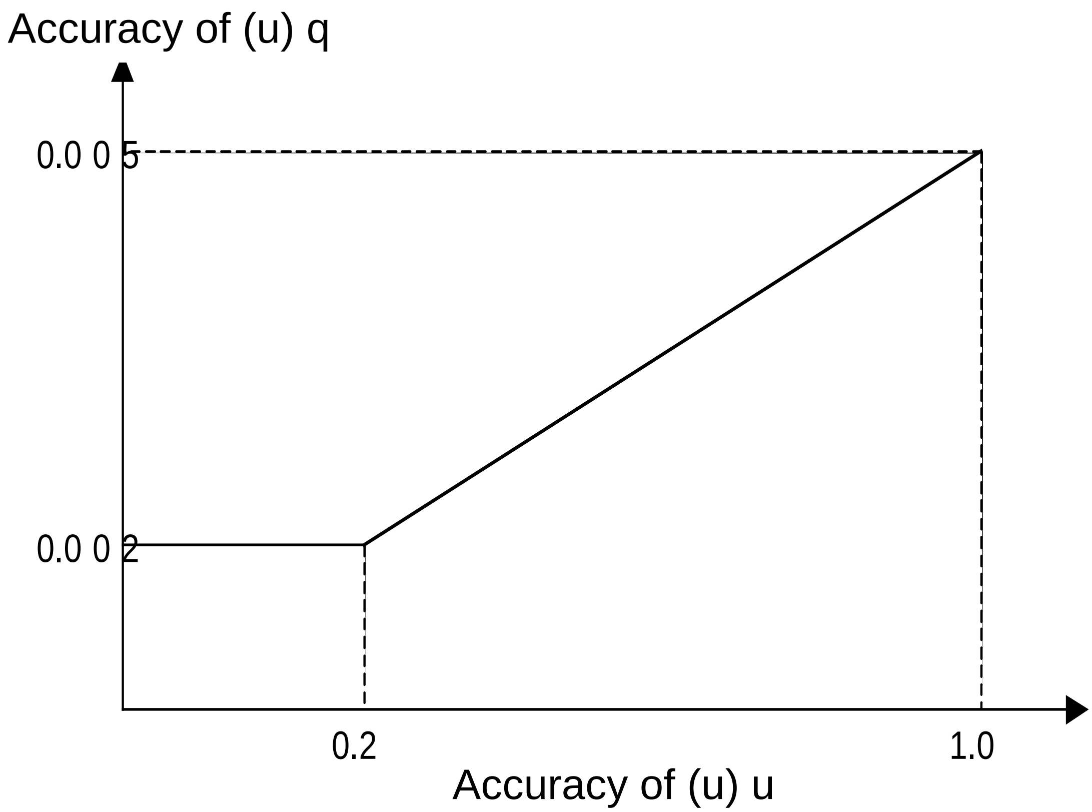

Figure 1.5-1 Functional variation of polarimetric accuracy with the measured value of q and u

2. CALIBRATION - THEORETICAL BASIS

The calibration of APS data requires coefficients that are generated as part of the sensor characterization and calibration pre-launch and also coefficients that are generated as the result of on-orbit observations of calibrators. This section introduces the calibration equation for APS data and defines the required calibration coefficients and their source.

2.1. APS Data

Here we describe the APS data and then introduce calibration equations that are required for measurements of this type. The Aerosol Polarimetry Sensor (APS) makes four measurements to analyze the linear polarization state of the incident radiation in each spectral band at each view angle (sector). This measurement approach uses identical paired optical assemblies that are designated as "telescopes" for brevity. One telescope (labeled 1) in each pair makes simultaneous measurements of the linearly-polarized intensity at azimuths of 0° and 90° with respect to the APS meridional plane of the scan, while the other telescope (labeled 2) simultaneously measures equivalent intensities at 45° and 135°. In reality the orientation of the Wollaston prisms will not be perfect and so the actual angle at which the polarizations are measured will have some small offset ε from the meridional plane, though the orthogonality will be almost perfect since it is determined by the crystalline structure of the Wollaston elements. The raw measurements are designated as R1L, R1R, R2L and R2R, respectively. The APS design provides measurements in nine spectral bands and thus a sector data record consists of nine sets of these four measurements, i.e., from 36 signal channels. During the DC-restoration period each of the 36 signal channels are DC-restored simultaneously to dark reference levels while the scanner views into a dark cavity. Following DC-restoration of the channels, measurement data are collected and stored while sequentially viewing: the dark reference cavity for pre-scene (post DC-restoration) dark reference samples designated as D1L, D1R, D2L and D2R; the unpolarized reference; the scene over an angular swath of 112° (-50° to +62° about nadir); the polarized reference; and the dark reference cavity for post-scene (pre-DC restoration for the next scan) dark reference samples designated as P1L, P1R, P2L and P2R.

The data in the four channels can therefore be modeled as:

$$I(0+\varepsilon_1) = C0 \times \left(R1L - D1Lm\right) \tag{1a}$$

$$I(90+\varepsilon_1) = C0 \times K1 \times \left(R1R - D1Rm\right) \tag{1b}$$

$$I(45+\varepsilon_2) = C0 \times C12 \times \left(R2L - D2Lm\right) \tag{1c}$$

$$I(135+\varepsilon_2) = C0 \times C12 \times K2 \times \left(R2R - D2Rm\right) \tag{1d}$$

where the *DXYm* terms are the mean dark counts for each channel. The reason for using four radiometric gain coefficients in this form will become clear as we discuss further the calibration approach and method.

2.1.1. APS System Model

In order to determine how the measurements in the four channels relate to the input Stokes vector it is necessary to model the primary sources of imperfection in a polarimeter of the APS type. The APS uses a pair of crossed mirrors to scan the field of view, the light then enters a refractive telescope before being analyzed by a Wollaston prism. In modeling the APS system we are concerned by the potential for the scan mirrors to introduce instrumental polarization, the fact that the lenses can introduce retardance (caused by stress) and imperfections in the Wollaston prisms. In fact the Wollaston prism performance is expected to be excellent and not a significant factor in degrading system performance, but the effects of depolarization and cross-talk can be subsumed in degraded polarizer performance for the sake of simplicity. The following Mueller matrices are therefore needed.

The primary source of instrumental polarization is expected to be mismatches between the APS mirrors. The Mueller matrix for a pair of crossed mirrors is

$$\mathbf{M}_m = R\begin{pmatrix} \cosh(\eta) & \sinh(\eta) & 0 & 0 \\ \sinh(\eta) & -\cosh(\eta) & 0 & 0 \\ 0 & 0 & -\cos(\Delta) & -\sin(\Delta) \\ 0 & 0 & -\sin(\Delta) & \cos(\Delta) \end{pmatrix} \tag{2}$$

where

$$\begin{aligned} R &= \sqrt{R_p R_p' R_s R_s'} \\ \eta &= \frac{1}{2}\left[\ln\left(\frac{R_s'}{R_s}\right) - \ln\left(\frac{R_p'}{R_p}\right)\right] \\ \Delta &= (\varepsilon_p - \varepsilon_s) - (\varepsilon_p' - \varepsilon_s') \end{aligned} \tag{3}$$

and

$$\begin{aligned} R_{s,p} &= \left|r_{s,p}\right|^2 \\ \varepsilon_{s,p} &= \arg(r_{s,p}) \end{aligned} \tag{4}$$

with $r_{s,p}$ being the complex reflectance for the s and p orientations of the electric field at the first mirror and the reflectance at the second mirror is defined by the same parameters but with a prime to indicate the potentially different properties at the second mirror. For Al mirrors at 630 nm illuminated at 45° the magnitude of ε_p- ε_s is around 10°. It is apparent that, apart from the inversion of Q and U by the double reflection, the magnitude of off-diagonal elements in the Muller matrix of the mirror system is determined by how well the mirrors are matched in the magnitude and phase of their reflections. For a linear retarder the Mueller matrix is

$$\mathbf{M}_r = \begin{pmatrix} 1 & 0 & 0 & 0 \\ 0 & 1 & 0 & 0 \\ 0 & 0 & \cos\delta & -\sin\delta \\ 0 & 0 & \sin\delta & \cos\delta \end{pmatrix} \tag{5}$$

where δ is the phase shift between two linear polarization components and a polarizer can be modeled as

$$\mathbf{M}_p = \frac{1}{2}\begin{pmatrix} p_x^2 + p_y^2 & p_x^2 - p_y^2 & 0 & 0 \\ p_x^2 - p_y^2 & p_x^2 + p_y^2 & 0 & 0 \\ 0 & 0 & 2p_x p_y & 0 \\ 0 & 0 & 0 & 2p_x p_y \end{pmatrix} \tag{6}$$

where p_x and p_y are the field transmission factors for the x and y components of the electric field. This matrix can be rewritten in a more useful form as

$$\mathbf{M}_p = \frac{p_x^2 + p_y^2}{2}\begin{pmatrix} 1 & \frac{e-1}{e+1} & 0 & 0 \\ \frac{e-1}{e+1} & 1 & 0 & 0 \\ 0 & 0 & \frac{2\sqrt{e}}{e+1} & 0 \\ 0 & 0 & 0 & \frac{2\sqrt{e}}{e+1} \end{pmatrix} \tag{7}$$

where e is the extinction ratio (of x and y intensities). In order to model the effects of the mirrors, lens retardance and the analysis of the Stokes vector by the Wollaston prism it is necessary to express the Mueller matrices for these elements in arbitrary frames of reference. Rotations of elements described by Mueller matrices are given by the expression

$$\mathbf{M}' = \mathbf{R}(-\alpha)\mathbf{M}\mathbf{R}(\alpha) \tag{8}$$

where α is the rotation angle and the rotation matrix R is given by

$$\mathbf{R}(\alpha) = \begin{pmatrix} 1 & 0 & 0 & 0 \\ 0 & \cos 2\alpha & \sin 2\alpha & 0 \\ 0 & -\sin 2\alpha & \cos 2\alpha & 0 \\ 0 & 0 & 0 & 1 \end{pmatrix} \tag{9}$$

The Mueller matrix for the crossed mirrors in an arbitrary frame is given by the expression

$$\mathbf{M}_m = R\cosh(\eta)\begin{pmatrix} 1 & \cos(2\alpha)\tanh(\eta) & \sin(2\alpha)\tanh(\eta) & 0 \\ \cos(2\alpha)\tanh(\eta) & -1+\sin^2(2\alpha)\xi & -\sin(2\alpha)\cos(2\alpha)\xi & \sin(2\alpha)\beta \\ \sin(2\alpha)\tanh(\eta) & -\sin(2\alpha)\cos(2\alpha)\xi & -1+\cos^2(2\alpha)\xi & -\cos(2\alpha)\beta \\ 0 & \sin(2\alpha)\beta & -\cos(2\alpha)\beta & 1-\xi \end{pmatrix} \tag{10}$$

where

$$\xi = \frac{\cosh(\eta) - \cos(\Delta)}{\cosh(\eta)} \tag{11}$$

and

$$\beta = \frac{\sin(\Delta)}{\cosh(\eta)}. \tag{12}$$

The Mueller matrix for a retarder in an arbitrary orientation is

$$\mathbf{M}_r = \begin{pmatrix} 1 & 0 & 0 & 0 \\ 0 & \cos^2(2\alpha)+\sin^2(2\alpha)\cos(\delta) & \sin(2\alpha)\cos(2\alpha)[1-\cos(\delta)] & \sin(2\alpha)\sin(\delta) \\ 0 & \sin(2\alpha)\cos(2\alpha)[1-\cos(\delta)] & \sin^2(2\alpha)+\cos^2(2\alpha)\cos(\delta) & -\cos(2\alpha)\sin(\delta) \\ 0 & -\sin(2\alpha)\sin(\delta) & \cos(2\alpha)\sin(\delta) & \cos(\delta) \end{pmatrix} \tag{13}$$

and for a polarizer in an arbitrary orientation the expression is

$$\mathbf{M}_p = \frac{p_x^2 + p_y^2}{2}\begin{pmatrix} 1 & \cos(2\alpha)\frac{e-1}{e+1} & \sin(2\alpha)\frac{e-1}{e+1} & 0 \\ \cos(2\alpha)\frac{e-1}{e+1} & \cos^2(2\alpha)+\sin^2(2\alpha)\frac{2\sqrt{e}}{e+1} & \sin(2\alpha)\cos(2\alpha)(1-\frac{2\sqrt{e}}{e+1}) & 0 \\ \sin(2\alpha)\frac{e-1}{e+1} & \sin(2\alpha)\cos(2\alpha)(1-\frac{2\sqrt{e}}{e+1}) & \sin^2(2\alpha)+\cos^2(2\alpha)\frac{2\sqrt{e}}{e+1} & 0 \\ 0 & 0 & 0 & \frac{2\sqrt{e}}{e+1} \end{pmatrix}. \tag{14}$$

The mirror mismatching terms η and Δ, together with the retardance δ are expected to be sufficiently small that those terms that are quadratically small can be neglected. If we make this approximation and combine the Mueller matrices for the crossed mirrors with that for the retarder, which represents a model of the effects of stress birefringence on the lenses, we find that the Stokes vector at the output of the lenses is

$$\begin{bmatrix} I' \\ Q' \\ U' \\ V' \end{bmatrix} = \begin{bmatrix} I + \tanh(\eta)[\cos(2\alpha_m)Q + \sin(2\alpha_m)U] \\ \cos(2\alpha_m)\tanh(\eta)I - Q + E_{q1} + E_{q2} \\ \sin(2\alpha_m)\tanh(\eta)I - U + E_{u1} + E_{u2} \\ V' \end{bmatrix} \tag{15}$$

where the error terms are given by the expressions

$$\begin{aligned} E_{q1} &= \frac{\sin(\Delta)\sin(\delta)}{\cosh(\eta)}\sin(2_{\alpha r}[Q\sin(2\alpha_m) - U\cos(2\alpha_m)] \\ E_{q2} &= \left[\sin(2\alpha_m)\frac{\sin(\Delta)}{\cosh(\eta)} + \sin(\delta)\sin(2\alpha_r)\right]V \\ E_{u1} &= \frac{\sin(\Delta)\sin(\delta)}{\cosh(\eta)}\sin(2_{\alpha r}[U\cos(2\alpha_m) - Q\sin(2\alpha_m)] \\ E_{u2} &= \left[-\cos(2\alpha_m)\frac{\sin(\Delta)}{\cosh(\eta)} - \sin(\delta)\cos(2\alpha_r)\right]V \end{aligned} \tag{16}$$

The terms E_{q1} and E_{u1} can be neglected for a sensor such as APS because they are quadratically small in the retardance and mirror matching errors. The terms E_{q2} and E_{u2} although linear in mirror matching and retardance errors are quadratically small compared with the other terms since V is at least two orders of magnitude smaller than Q and U for naturally illuminated scenes on the Earth. The model for the Stokes vector that arrives at the Wollaston prisms is therefore

$$\begin{bmatrix} I' \\ Q' \\ U' \\ V' \end{bmatrix} = \begin{bmatrix} I + q_{inst}Q + u_{inst}U \\ q_{inst}I - Q \\ u_{inst}I - U \\ V' \end{bmatrix} \tag{17}$$

where we have made the identification $q_{inst}=\tanh(\eta)\cos(2\alpha_m)$ and $u_{inst}=\tanh(\eta)\sin(2\alpha_m)$. The measurements in the four channels are therefore related to the incident Stokes vectors as follows

$$I(0+\varepsilon_1) = \frac{I + q_{inst}Q + u_{inst}U + \frac{e_1-1}{e_1+1}\left\{\cos(2\varepsilon_1)[q_{inst}I - Q] + \sin(2\varepsilon_1)[u_{inst}I - U]\right\}}{2} \tag{18a}$$

$$I(90+\varepsilon_1) = \frac{I + q_{inst}Q + u_{inst}U - \frac{e_1-1}{e_1+1}\left\{\cos(2\varepsilon_1)[q_{inst}I - Q] + \sin(2\varepsilon_1)[u_{inst}I - U]\right\}}{2} \tag{18b}$$

$$I(45+\varepsilon_2) = \frac{I + q_{inst}Q + u_{inst}U + \frac{e_2-1}{e_2+1}\left\{-\sin(2\varepsilon_2)[q_{inst}I - Q] + \cos(2\varepsilon_2)[u_{inst}I - U]\right\}}{2} \tag{18c}$$

$$I(135+\varepsilon_2) = \frac{I + q_{inst}Q + u_{inst}U - \frac{e_2-1}{e_2+1}\left\{-\sin(2\varepsilon_2)[q_{inst}I - Q] + \cos(2\varepsilon_2)[u_{inst}I - U]\right\}}{2} \tag{18d}$$

where the extinction ratios of the two Wollaston prisms (e_1 and e_2) can be different. Let us now form sums and differences of these four quantities viz.,

$$I(0+\varepsilon_1) + I(90+\varepsilon_1) = I\left\{1 + p_{inst}\,p\cos[2(\chi_{inst} - \chi)]\right\} \tag{19a}$$

$$I(0+\varepsilon_1) - I(90+\varepsilon_1) = \frac{e_1-1}{e_1+1} I\left\{\tilde{q}_{inst} - \cos(2\varepsilon_1)q - \sin(2\varepsilon_1)u\right\} \tag{19b}$$

$$I(45+\varepsilon_2) + I(135+\varepsilon_2) = I\left\{1 + p_{inst}\,p\cos[2(\chi_{inst} - \chi)]\right\} \tag{19c}$$

$$I(45+\varepsilon_2) - I(135+\varepsilon_2) = \frac{e_2-1}{e_2+1} I\left\{\tilde{u}_{inst} + \sin(2\varepsilon_2)q - \cos(2\varepsilon_2)u\right\} \tag{19d}$$

where the instrumental polarizations are now defined to be in the plane of the Wollaston prisms rather than the ideal orientation

$$\begin{aligned}\tilde{q}_{inst} &= \cos(2\varepsilon_1) q_{inst} + \sin(2\varepsilon_1) u_{inst} \\ \tilde{u}_{inst} &= \cos(2\varepsilon_2) u_{inst} - \sin(2\varepsilon_2) q_{inst}\end{aligned} \tag{20}$$

and we define $q=Q/I$, $u=U/I$, $p=(Q^2+U^2)^{0.5}/I$, $p_{inst}=(q_{inst}{}^2+u_{inst}{}^2)^{0.5}$, $\tan(2\chi_{inst})=u_{inst}/q_{inst}$ and $\tan(2\chi)=u/q$. A method for accurately estimating I, q and u in the presence of instrumental polarization can be derived by examining the following non-linear equations,

$$\frac{I(0+\varepsilon_1)-I(90+\varepsilon_1)}{I(0+\varepsilon_1)+I(90+\varepsilon_1)} \times \alpha_q \times \xi(p) - \tilde{q}_{inst} \approx \{-\cos(2\varepsilon_1) q - \sin(2\varepsilon_1) u\} \tag{21}$$

and

$$\frac{I(45+\varepsilon_2)-I(135+\varepsilon_2)}{I(45+\varepsilon_2)+I(135+\varepsilon_2)} \times \alpha_u \times \xi(p) - \tilde{u}_{inst} \approx \{\sin(2\varepsilon_2) q - \cos(2\varepsilon_2) u\} \tag{22}$$

where the scale factors α_q and α_u are defined to be

$$\alpha_q = \frac{e_1+1}{e_1-1} \tag{23}$$

and

$$\alpha_u = \frac{e_2+1}{e_2-1} \tag{24}$$

and the polarization dependent factor x is given by the expression

$$\xi(p) = \{1 + p_{inst}\, p \cos[2(\chi_{inst} - \chi)]\} \tag{25}$$

These equations can be solved iteratively in the following way. Let

$$x_i = \frac{I(0+\varepsilon_1)-I(90+\varepsilon_1)}{I(0+\varepsilon_1)+I(90+\varepsilon_1)} \times \alpha_q \times \xi(p_i) - \tilde{q}_{inst} \tag{26}$$

and

$$y_i = \frac{I(45+\varepsilon_2)-I(135+\varepsilon_2)}{I(45+\varepsilon_2)+I(135+\varepsilon_2)} \times \alpha_u \times \xi(p_i) - \tilde{u}_{inst} \tag{27}$$

then

$$\begin{bmatrix} q_i \\ u_i \end{bmatrix} = \frac{-1}{\cos[2(\varepsilon_1-\varepsilon_2)]} \begin{bmatrix} \cos(2\varepsilon_2) & -\sin(2\varepsilon_1) \\ \sin(2\varepsilon_2) & \cos(2\varepsilon_1) \end{bmatrix} \begin{bmatrix} x_i \\ y_i \end{bmatrix} \tag{28}$$

with

$$\begin{aligned}&\xi(p_0) = 1\\&\xi(p_i) = \{1 + p_{inst}\, p_{i-1} \cos[2(\chi_{inst} - \chi_{i-1})]\}\end{aligned} \qquad (29)$$

For the required instrumental polarization level of less than 1% convergence to an accuracy of less than 0.1% will occur in two iterations. The form of calibration outlined above has been used on data taken with the Research Scanning Polarimeter (RSP) with excellent results (<0.1%, Cairns et al. 1999). After testing the as built Aerosol Polarimetry Sensor it has become clear that the instrumental polarization is so low in all bands except the 410 nm band that the correction is negligible (<<0.1%). In the 410 nm band the instrumental polarization is still low enough (<0.5%) that it can be corrected without iteration, but it depends on view angle and there is instrumental polarization present in the viewing direction that provides the relative gain coefficients. The relative gain coefficients in the 410 nm band therefore need the correction to the apparent gain coefficient applied as indicated in Eq. (E) of Section 4.1. The tabulated values of the instrumental polarization as a function of viewing angle are given in Appendix A.

In practice, because the relative phase of *q* and *u* (i.e. the difference between ε_1, or ε_2) is better known than the absolute values of either ε_1, or ε_2 equation (28) is re-written in the form

$$\begin{bmatrix} q_i \\ u_i \end{bmatrix} = \begin{bmatrix} \cos(2\Delta_\varepsilon) & -\sin(2\Delta_\varepsilon) \\ \sin(2\Delta_\varepsilon) & \cos(2\Delta_\varepsilon) \end{bmatrix} \frac{1}{\cos(4\delta_\varepsilon)} \begin{bmatrix} \cos(2\delta_\varepsilon) & -\sin(2\delta_\varepsilon) \\ -\sin(2\delta_\varepsilon) & \cos(2\delta_\varepsilon) \end{bmatrix} \begin{bmatrix} x_i \\ y_i \end{bmatrix} \qquad (30)$$

where

$$\begin{aligned}\varepsilon_1 &= \Delta_\varepsilon + \delta_\varepsilon\\ \varepsilon_2 &= \Delta_\varepsilon - \delta_\varepsilon\end{aligned} \qquad (31)$$

and the factor of negative one has been subsumed into the absolute orientation rotation. This formally separates the correction for the Wollaston prisms being incorrectly aligned with respect to one another from the correction for the absolute orientation of the Wollaston prisms. Since Fourier analysis of a rotated ultra-high efficiency wire grid polarizer is used to determine the relative phase of *q* and *u*, while the absolute orientation of polarization is determined using a Suprasil 300 plate oriented to Brewster's angle this separation also make practical sense. The relative orientation of the Wollaston prisms, $2\delta_\varepsilon$, is determined for primary and redundant electronics, for the thermal/vacuum hot, cold and acceptance conditions and also as a function of view angle. These calibration coefficients are tabulated in Appendix A.

The values for the absolute orientation correction, $2\Delta_\varepsilon$, are only determined for the primary side electronics since they provide an absolute reference against which to correct the orientation of the wire-grid polarizer used to determine the relative orientation of the Wollaston prisms and are also given in Appendix A. In addition to a polarization orientation rotation that is determined for the nadir view the polarization azimuth is also rotated in a fixed, repeatable manner by the rotation of the APS scanner. This rotation also needs to be corrected for and this corrected rotation is given by

$$2\Delta_\varepsilon' = 2[\Delta_\varepsilon + (115\text{-isector})2\pi/768] \qquad (32)$$

where 115 is the Earth viewing sector index (starting at 0) of the nominal nadir view for which Δ_ε is determined and the factor $2\pi/768$ indicates that the APS scan is broken into 768 elements separated by 8.18 mrad.

2.1.2. APS Calibration Coefficients

We can now enumerate the APS calibration coefficients and identify their sources. The table below provides this information.

Coefficient	Source	Accuracy
K1, K2	Unpolarized reference on orbit. *(Section 3)*	<0.1%
$\alpha_q(p_0)$, $\alpha_u(p_0)$	Polarized reference on orbit. *(Section 3)*	<0.1%
C12	Comparison of measurements from telescope pairs on orbit. *(Section 4)*	<0.1%
C0	Solar reference and lunar calibration. *(Section 4)*	<5%
q_{inst}, u_{inst}	Pre-launch characterization. *(APS Calibration and Characterization Plan)*	<0.1%
ε_1, ε_2	Pre-launch characterization. *(APS Calibration and Characterization Plan)*	<0.05°

Table 2.1.2-1. Enumeration and identification of sources for APS calibration coefficients.

2.1.3. APS Calibration Implementation

The actual calculations that are performed on the APS data in order to obtain calibrated values of *I*, *Q*, *U*, *p* and χ are given in this section.

1. Calculate mean dark reference value from the sixteen dark reference values available after the DC restore operation.
   a) Input: APS raw data.
   b) Output: Mean dark reference values, generally designated as DXYm where X can take the value 1 or 2 and Y can take the value L or R. The Pre_DXY values are from the pre-DC restore observations of the dark reference and the Post_DXY values are from the post-DC restore observations of the dark reference.

c) Method:

$$DXYm = \frac{\sum_{i=pre\_lo}^{pre\_hi} Pre\_DXY(i) + \sum_{i=post\_lo}^{post\_hi} Post\_DXY(i)}{(pre\_hi - pre\_lo + 1) + (post\_hi - post\_lo + 1)} \quad \text{(A)}$$

2. Calculate dark corrected intermediate results SXY.
   a) Input: APS raw data and average dark counts
   b) Output: Dark corrected digital numbers
   c) Method:

$$SXY = RXY - DXYm \quad \text{(B)}$$

3. Calculate intermediate results, ΣX and δX.
   a) Input: APS raw data, K1, K2 calibration coefficients.
   b) Output: Intermediate results that are used in the determination of *I*, *q* and *u* and also in the evaluation of the calibration coefficients C12 and C0.
   c) Method:

$$\Sigma 1 = S1L + K1.S1R \quad \text{(C)}$$

$$\Sigma 2 = S2L + K2.S2R \quad \text{(D)}$$

$$\delta 1 = \frac{S1L - K1.S1R}{\Sigma 1} \quad \text{(E)}$$

$$\delta 2 = \frac{S2L - K2.R2R}{\Sigma 2} \quad \text{(F)}$$

4. Calculate *q*, *u*, *p* and χ and $\xi(p)$. Correct for misalignment of Wollastons, instrumental polarization and instrumental depolarization.
   a) Input: δ1, δ2, α_q, α_u, q_{inst} and u_{inst} calibration coefficients.
   b) Output: *q*, *u*, *p* and χ together with ξ(p) that is required for the calculation of *I*.
   c) Method: Equations 21 and 22, 26 and 27 can be rewritten in terms of δ1 and δ2 and are independent of the absolute radiometric calibration coefficient C0, or the inter-telescope radiometric calibration coefficient C12. The iterative solution is then implemented as follows:
      i) Initial value for $\xi(p)$ is:

$$\xi(p_0) = 1 \quad \text{(G)}$$

      ii) Iteration starts with index 0 and loops over the following equations. The iteration is terminated when $|\ln[\xi(p_i)/\xi(p_{i-1})]| < 0.001$. Thus if the instrumental polarization is less than 0.1% there will be no iteration, just a first order correction.

$$x_i = \delta 1 \times \alpha_q \times \xi(p_i) - \tilde{q}_{inst} \quad \text{(H)}$$

$$y_i = \delta 2 \times \alpha_u \times \xi(p_i) - \tilde{u}_{inst} \quad \text{(I)}$$

$$\begin{bmatrix} q_i \\ u_i \end{bmatrix} = \begin{bmatrix} \cos(2\Delta_\varepsilon) & -\sin(2\Delta_\varepsilon) \\ \sin(2\Delta_\varepsilon) & \cos(2\Delta_\varepsilon) \end{bmatrix} \frac{1}{\cos(4\delta_\varepsilon)} \begin{bmatrix} \cos(2\delta_\varepsilon) & -\sin(2\delta_\varepsilon) \\ -\sin(2\delta_\varepsilon) & \cos(2\delta_\varepsilon) \end{bmatrix} \begin{bmatrix} x_i \\ y_i \end{bmatrix} \quad \text{(J)}$$

$$p_i = \sqrt{q_i^2 + u_i^2}$$
$$\tan(2\chi_i) = {u_i}/{q_i} \tag{K}$$
$$\xi(p_i) = \{1 + p_{inst} p_i \cos[2(\chi_{inst} - \chi_i)]\} \tag{L}$$

5. Calculate *I*. Correct for instrumental polarization.
    a) Input: ΣX and the C0, C12, and ξ(*p*) calibration coefficients.
    b) Output: I calculated separately for each telescope.
    c) Method: If we rewrite equations 19a and 19c in terms of the intermediate results we already calculated we find that in order to determine the intensity we need to perform the following calculations:

$$I = \frac{I(0+\varepsilon_1) + I(90+\varepsilon_1)}{\xi(p)} = \frac{C0 \times \Sigma 1}{\xi(p)} \tag{M}$$
$$I = \frac{I(45+\varepsilon_2) + I(135+\varepsilon_2)}{\xi(p)} = \frac{C0 \times C12 \times \Sigma 2}{\xi(p)} \tag{N}$$

    d) Additional Calculation: Since in the retrieval of aerosol and cloud properties we are primarily interested in the reflectance we will also calculate the normalized radiance *i*, which is a closely related quantity, which we will define to be

$$i = \frac{I\pi}{F_0}. \tag{O}$$

    where F_0 is the APS band integrated solar irradiance derived from ground-based spectral calibration measurements and a solar spectral irradiance data set [Lean 2002]. The values of F0 used in generating the normalized radiance are given in Appendix A.

3. RADIOMETRIC CALIBRATION

In this section we describe how the radiometric calibration coefficients that are generated on orbit are calculated and used in the calibration process.

3.1. Introduction

The on-orbit radiometric calibration of the APS is required to meet the science requirements for retrieving aerosols properties over land and ocean. The APS will be radiometrically calibrated using a solar reference that consists of a spaceflight grade Spectralon plaque that has its bidirectional reflectance distribution function calibrated prior to launch and that is protected by a one-time deployable cover. The cover of the solar reference will be opened shortly after the APS performs a lunar calibration and the first view of the solar reference will serve as the defining reflectance standard for the mission. Once the cover has opened the Spectralon plaque will tend to degrade and its reflectance will decrease in an unpredictable manner. Lunar calibration will then be used to maintain the APS radiometric scale.

3.2. Discussion

Experience with diffusers on previous satellite instruments has led to the theory that diffuser degradation on orbit is caused by the coating of the panel with photolyzed organic materials that are outgassed from the spacecraft. This is consistent with the observation that the degradation is systematically larger with decreasing wavelength. This accumulation of organic materials is expected to be temporally smooth with the diffuser slowly degrading over its lifetime. This type of secular change is shown in Figure 3.2-1 below that was provided by Raytheon SBRS.

Although this type of degradation means that a diffuse target cannot be used as an absolute reflectance scale after more than a relatively short period on orbit it can nonetheless be used to evaluate radiometric stability over the shorter term. This type of evaluation is essential if calibrations using lunar views, or vicarious calibrations are to be put in the appropriate context. Even the MODIS spectralon diffuser shown in Figure 1 shows fluctuations on short time scales of less than 1% and the behavior shown in Figure 3.2-2 by the SeaWiFs diffuser panel is more typical of what is generally found to occur to diffuser reflectors in the on orbit environment. Of particular relevance to the use of diffuse reflectance standards is the need to adequately characterize their bidirectional reflectance distribution function (BRDF), so that variations in solar view angle are not erroneously inferred to be diffuser variations. It is also essential to characterize the BRDF if the diffuse reflector is to be used to establish the initial on orbit radiometric scale.

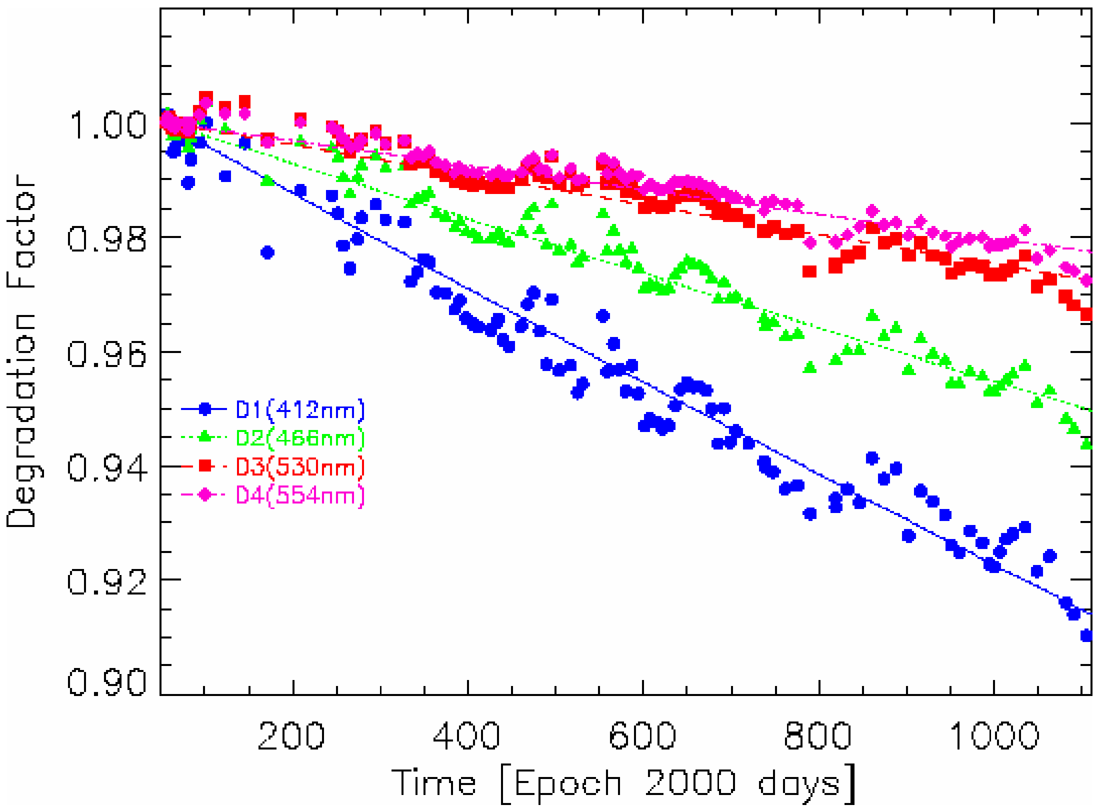

Figure 3.2-1 Evaluation of MODIS spectralon diffuser provided by Raytheon SBRS.

One means for tracking radiometric stability once a sensor is on orbit is to view the moon. Although using a diffuse reflector to establish the calibration scale at “first light” is essential for a sensor with the spatial resolution of APS, once the scale is established the stability of the sensor can be tracked using these lunar views. The moon is photometrically stable at a level of roughly 10^{-9} per year and now has been observed for more than 5 years by the The RObotic Lunar Observatory (ROLO) Project. This project has obtained approximately 85,000 lunar images and more than 10^6 star images in 32 bands (23 VNIR, 9 SWIR). This library of images provides substantial coverage in the 3-parameter phase+libration space, however, large libration gaps exist for any specific phase. Nonetheless, provided APS views the moon at similar points in its phase over the duration of the mission, these views will be sufficient in themselves to check the stability of the sensor.

In Table 3.2-1 we show the current APS radiometric calibration requirements together with the locations of spectral bands that are available in the ROLO data base. It is clear from the excellent coincidence of APS and ROLO spectral bands that these spectral differences will not be a significant issue in determining the relative spectral accuracy (RSA) of the APS bands if the ROLO data base is being used. Alternatively the spectral variation of the diffuser can be tracked by APS lunar measurements at a fixed lunar phase, which would also allow the RSA to be determined independent of the ROLO data base. Thus, lunar views can be used to determine RSA provided adequate bore sighting of all telescopes is achieved.

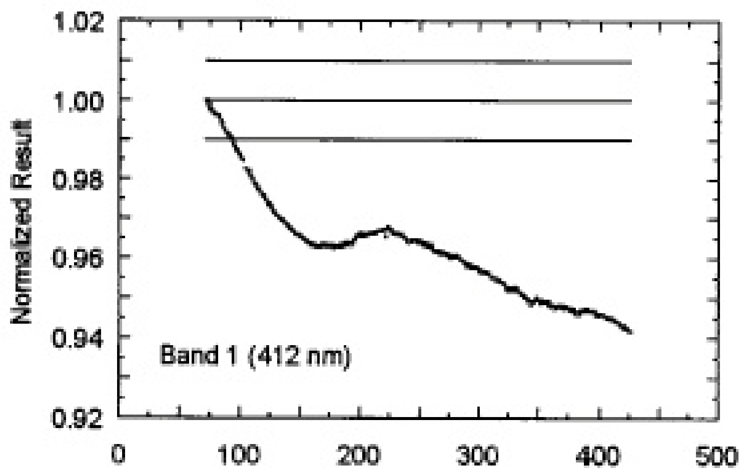

Figure 3.2-2. Stability of SeaWiFs diffuser.

Band	λ (nm)	Radiometric (Reflectance-based)			ROLO	
		Absolute Accuracy (1 σ)	Relative Spectral Accuracy (1σ)	Precision (1σ)	Center (nm)	Width (nm)
P1	412	5% or 1 DN whichever is larger	<1%	0.8%	412.7	12.5
P2	443	5% or 1 DN whichever is larger	<1%	0.8%	441.8	9.6
P3	555	5% or 1 DN whichever is larger	<1%	0.8%	554.9	18.1
P4	672	5% or 1 DN whichever is larger	<1%	0.8%	666.7	8.3
P5	865	5% or 1 DN whichever is larger	<1%	0.8%	867.7	13.9
P6	910	5% or 1 DN whichever is larger	<1%	1.0%	934.6	17.6
P7	1378	8% or 1 DN whichever is larger	<1%	0.8%	1246.5/ 1542.7	23.3/48.6
P8	1610	5% or 1 DN whichever is larger	<1%	0.8%	1637.8	23.4
P9	2250	5% or 1 DN whichever is larger	<1%	0.8%	2256.3	48.2

Table 2. Radiometric performance specified in the APS SMRD together with the ROLO bands that are closest to the APS bands.

3.3. *Alternative Methods for Radiometric Calibration of APS*

3.3.1. *Reflectance Based*

	Atmosphere	Reflector	Transmission	DN for site
Lunar	N/A	1.0 (Note 1)	N/A	2.0
OBC	N/A	2.5 (Note 2)	N/A	1.0
Vicarious	3.8	2.1	1.9	1.0

Table 3.3.1-1 Estimation of magnitudes of uncertainty for different calibration approaches in %.

Notes:

1. No established absolute irradiance scale for lunar observations currently exists. 0.96% is maximum uncertainty in BRDF model of moon. NIST and USGS are currently pursuing this.
2. This value is only valid at “first light” before reflector degrades.

Lunar views, a solar reference and vicarious calibrations all use forms of reflectance based calibration. It is just that in the case of solar reference and lunar views the atmosphere is not a problem. However the absolute reflectance of the target is a problem for lunar and solar reference views while for vicarious calibrations this uncertainty can be minimized.

The use of vicarious calibration for the APS sensor is not trivial because of the large sensor footprint. This will require the use of an aircraft making low altitude measurements to adequately characterize a sufficiently large area of the surface in order to apply this approach. This method can be complemented by high altitude measurements that would allow a direct radiance based calibration as discussed below. The overall accuracy of a vicarious calibration is typically 5% under good conditions. The primary method for reducing this uncertainty would be to make ground based sky radiometry and polarimetry measurements to reduce the uncertainties in size distribution and refractive index of aerosols. These measurements would reduce the overall uncertainty of a vicarious calibration to 3.3%. Nonetheless some form of diffuse reflectance calibrator is essential to determine sensor stability over shorter periods and establish an initial calibration scale once on orbit

3.3.2. Radiance Based

Radiance based calibration has the potential to be the most accurate form of calibration and is the preferred radiance standard at NIST. There are two types of radiance based calibration that will be available to APS. The first is cross-calibration with other sensors such as MODIS or VIIRS and the second is through the use of field experiments where a well calibrated radiometer is flown at high altitude to obtain data at the same time as an APS overpass.

The accuracy of the first type of radiance based calibration is determined by the accuracy of the sensor which is being used as the source for cross-calibration and by the relative viewing geometry and degree of simultaneity of acquisitions by the two sensors. These have been summarized as follows by Slater et al. (1996):

1) Same geometric instantaneous field of view (GIFOV) and spectral bands and simultaneous acquisition.
2) Similar spectral bands and imaging the same scene simultaneously, but with different GIFOVs.
3) Same GIFOVs but different viewing geometry with near simultaneity (i.e. a few minutes similar to ASTER and MISR).
4) Similar spectral bands and IFOVs but not simultaneous.

These four cases are estimated to have transfer uncertainties of 1, 2, 5 and 7-9 % one sigma respectively. The case of APS would probably correspond to a variation on case 3) with different IFOV and viewing geometry but simultaneous acquisition. Given that APS measures the BRDF the estimated uncertainty for transfer in this case would be 2.5% (2% for difference in GIFOV and 1.5% for BRDF effects). Thus if the radiometric accuracy of MODIS is 3% then the accuracy of the radiometric scale transferred to APS would be expected to be 4%. Similarly if the radiometric accuracy of VIIRS is 2% then the accuracy of the radiometric scale transferred to APS would be expected to be 3.2%.

The accuracy of the second type of radiance based calibration is determined by the accuracy of the high altitude radiometer and the quality of the measurements made by the radiometer at high altitude (stability, pointing, spatial sampling, simultaneity). These two components of the error budget are on the order of 2.5% and 1.5% respectively yielding a 3% radiometric accuracy for this form of calibration when it is performed correctly.

3.4. Summary of Radiometric Calibration Approach

The planned approach for APS calibration in order to meet the SMRD radiometric calibration requirements is to have a one-time deployable diffuse reflectance based calibrator that will establish the on orbit reflectance scale at the beginning of the mission. The reflectance calibrator must have its BRF and BRDF adequately characterized so that the absolute calibration will meet requirements and so that the calibrator can be effectively used over the course of the entire mission. This means the BRDF must be characterized over an angular range consistent with all the view geometries that are expected for the mission.

The absolute and relative spectral accuracy of the APS will be maintained by using lunar views to track the degradation of the reflectance calibrator, and/or by using lunar views and the ROLO data base. In practice it is expected that both methods will be used. The moon is intrinsically stable and the current stability of the ROLO measurements over a period of 5 years from a ground-based telescope is better than 0.5%.

Radiance-based calibration using comparisons with observations from a high altitude aircraft will be used to verify the APS radiometric/reflectance scale.

3.5. Solar Reference Calibration

The APS calibration approach requires looking at the solar calibrator within a few minutes of opening the door. We assume that the bidirectional reflectance distribution function (BRDF) of the Spectralon will not have changed since the ground-based calibration and characterization. It is therefore important that the Spectralon is carefully treated and not allowed to be illuminated by UV, or contaminated during integration and test. The observed values of the intermediate functions introduced in equation (B) and (C) are related to the required calibration coefficients as follows:

$$C0 = \frac{\mu_{AOI} R_{Spec}(\theta_i, \theta_v, \Delta\phi) F_0}{\Sigma 1(SolCal)\, \pi D_{SE}^2} \tag{O}$$

and

$$C0 \times C12 = \frac{\mu_{AOI} R_{Spec}(\theta_i, \theta_v, \Delta\phi) F_0}{\Sigma 2(SolCal)\, \pi D_{SE}^2} \tag{P}$$

where F_0 is the APS band integrated solar irradiance, D_{SE} is the Sun-Earth distance and μ_{AOI} is the cosine of the angle of incidence of the solar beam on the Spectralon plaque. This defines the initial APS radiometric scale and lunar calibration will be made within a few orbits in order to provide an estimate of the effective disk reflectance of the moon.

3.6. Lunar Calibration

3.6.1. Lunar Calibration Maneuver

The Glory satellite will be flown in a sun-synchronous orbit with a nominal ascending node at 13:30 AM mean local time. A planned satellite maneuver which reorients the APS FOV to look at the moon after the satellite has passed the northern terminator of its orbit is outlined below:

1. At a lunar phase angle of 24±3° roughly 3 days before full moon, the spacecraft will roll to a target 1.0° away from the moon. This will take 250 seconds.
2. The ACS will then be commanded to perform a slew to a target 2.0° away on the other side of the moon at a rate of 0.0133 deg/sec. This will take 150 seconds.
3. The ACS will then be commanded to return to the original target 2.0° away on the other side of the moon at a rate of 0.0133 deg/sec. This will take 150 seconds.
4. The ACS will then be commanded to perform a slew to a target 1.5° away on the other side of the moon at a rate of 0.0133 deg/sec. This will take 150 seconds.
5. The ACS will then be commanded to perform a slew to a target 1.5° away on the other side of the moon at a rate of 0.0133 deg/sec. This will take 150 seconds.
6. When lunar sampling is complete, the spacecraft will roll back to its original nadir-pointing orientation. This will take 250 seconds.

The moon is approximately 0.5° in diameter when viewed from Earth orbit. The GIFOV of the APS is 8 mrad (0.46°) in diameter. The zig-zag maneuver described above will provide four sets of lunar radiance measurements that are oversampled in the roll direction with one hundred (100) measurements of the moon in each data set. This oversampling is necessary because of the marginal APS FOV filling provided by the moon.

A zig-zag maneuver ensures that the entire lunar image is captured during the scan. As the spacecraft "scans" the moon by rolling and the APS scans along-track, the moon is very slowly moved through the APS FOV in both the along-track and cross-track directions and this will ensure that there are multiple views with the moon centered in the APS FOV. In order to calculate an integrated lunar radiance we use a weighted average of the scans and sectors that provide the most uniform spatial integration across the moon. The weightings, c_k, are calculated based on the actual scan geometry projected onto the moon and the structure and spacing of the apodized APS IFOVs and provide the flattest field that is consistent with non-negative weights (i.e. the c_k are determined by a non-negative least squares estimate. The over-sampling is therefore corrected in this case by the use of the weights to create a uniform integrator. The integrated lunar radiance is then given by the expression

$$\bar{I}_k = \sum_{i=1,20;\, j=1,100} I_k(j,i) \qquad \text{(Q)}$$

where i denotes an index over sectors centered on peak lunar radiance, j denotes an index over the scans from start of the slow lunar roll until its end and k is an index over APS bands.

3.6.2. Lunar Calibration Correction Factors

Lunar calibration and stability tracking of the APS measurements assumes that the moon's brightness is constant. In order to ensure consistency, correction, or normalization, factors must be applied to the measurements of the moon that are collected. These factors include:

- Sun-moon distance
- Instrument-moon distance
- Lunar phase angle
- Libration

Each of these factors is discussed in the following sections.

3.6.2.1. Sun, Moon, Instrument Distances

Since neither the orbits of the Earth nor that of the moon are perfectly circular, the distances between the sun, Earth, and moon change over time. The amount of solar flux intercepted by the moon varies inversely with the square of the lunar distance from the sun, so the shorter the distance, the brighter the moon will appear. Similarly, the brightness of the moon observed by the APS will vary with the inverse square of its distance from the moon if the moon underfills the APS effective FOV which it does, by design, for the integrated lunar radiance. Care must therefore be taken to correct the integrated lunar radiance for the sun-moon distance and the moon-viewer distance. The equation used to do this is

$$\bar{I}_k' = \bar{I}_k \left(\frac{D_{SM}}{1AU} \right)^2 \left(\frac{D_{MV}}{384,400km} \right)^2 \qquad \text{(R)}$$

where D_{SM} is the sun-moon distance (AU) and D_{MV} is the moon-viewer distance (in km) and 384,400 km is the mean radius of the orbit of the moon around the Earth.

3.6.2.2. Oversampling Correction

The oversampling correction is a key aspect of using the moon to track stability. The IFOV of the APS instrument is not square like the one of the SeaWiFs instrument, nor is it as small as that of the SeaWiFs instrument. It is therefore necessary to analyze the oversampling correction to what we really want, which is the integrated lunar radiance, carefully. The estimated integrated radiance is related to the Fourier transform of the lunar radiance distribution $I(\eta,\nu)$ by the expression

$$\bar{I}_k' = \int g(\eta,\nu) I(\eta,\nu) \frac{\sin(\pi\nu\Delta_x N_x)}{\sin(\pi\nu\Delta_x)} \frac{\sin(\pi\eta\Delta_y N_y)}{\sin(\pi\eta\Delta_y)} d\nu d\eta \qquad \text{(S)}$$

where $g(\eta,\nu)$ is the Fourier transform of the apodized aperture function, N_x is the number of samples in the roll direction, N_y is the number of samples in the scan direction, Δ_x is the angular spacing of scans in the roll direction, Δ_y is the angular spacing of samples in the scan direction. If the sin(Nx)/sin(x) functions are effectively acting as delta functions and the sample spacing is fine enough that the aperture function band limits the integral in (S) which is achieved if $\Delta_M >> \Delta_X >> \Delta_M / N_x$ and $N_y >> 1$ then this expression takes on the more familiar form

$$I(0,0) = \bar{I}_k'' = \bar{I}_k' \frac{\Delta_x \Delta_y}{\Omega_{APS}} \qquad \text{(T)}$$

where we identify the Fourier transform of the lunar radiance distribution at zero frequency as the integrated lunar radiance that we are interested in and Ω_{APS} is the FOV of the apodized aperture. This approach assumes that the spacecraft rotation rate is well known during the maneuver, and would have to be slightly modified if the rate must also be estimated by using the phase of the FFT of the lunar radiance field to estimate the rates. Expression (T) reduces to equation (4) of Barnes et al. [2003] for the case of SeaWiFs.

3.6.2.3. Lunar Phase Angle and Libration Effects

The lunar phase angle is a significant factor, because the moon's brightness varies greatly depending on its phase. In order to be consistent, the calibration maneuver used for SeaWiFS, which uses lunar calibration, was consistently performed when the moon was approximately 7° from full. Initial calculations suggest that Glory will need to have a larger phase angle, up to three days from full (more than 30°), in order to avoid occulting the star-tracker(s). The opposition effect creates the only other significant restriction in what particular phase angle to choose. As Figure 3 shows, the rate of change in brightness of the lunar disk rapidly increases as the phase angle decreases below about 5° due to the opposition effect. This effect means that if there is even a very small change in phase angle from month to month, the change in brightness will be very significant and the correction factor to account for this variation will need to be very precise. At greater phase angles, the overall lunar irradiance decreases, but small variations in phase angle are less problematic. The smaller the phase angle, the brighter the moon will appear from the APS, but as long as the brightness is constant, the magnitude is not a crucial factor.

In modeling the effects of lunar phase angle and libration we will use the model for the effective disk reflectance of the moon developed by the USGS [Kieffer and Stone 2004, Stone, Kieffer, and Becker, 2003; Kieffer and Anderson 1998]. The effective disk reflectance is defined to be [Barnes et al. 2003]

$$\begin{aligned} A_k &= \frac{\pi \bar{I}_k''}{F_{0,k}} \times \frac{\Omega_{APS}}{\Omega_M} = \frac{\pi \bar{I}_k'}{F_{0,k}} \times \frac{\Delta_x \Delta_y}{\Omega_M} \\ A_k &= \frac{\pi \bar{I}_k}{F_{0,k}} \times \frac{\Delta_x \Delta_y}{\Omega_M} \times \left(\frac{D_{SM}}{1AU}\right)^2 \left(\frac{D_{MV}}{384,400km}\right)^2 \end{aligned} \qquad \text{(U)}$$

where $F_{0,k}$ is the solar irradiance at 1AU, Ω_M is the solid angle of the moon at 384,400 km (6.4236×10^{-5} sr) and Ω_{APS} is the solid angle of the APS (5×10^{-5} sr). The effective disk reflectance can then be tied directly to the initial solar calibration observations and the reflectance of the Spectralon plaque by substituting in the quantity *C0* x *ΣX* for *I* in the expression for the integrated lunar radiance and using equation (O) for the calibration coefficient viz.,

$$A_k^{APS} = R_{Spec,k}(\theta_i,\theta_v,\Delta\phi)\times\frac{\sum_{i,j}\Sigma 1_k(i,j)}{\Sigma 1_k(SolCal)}\times\mu_{AOI}\times\frac{\Delta_x\Delta_y}{\Omega_M}\times\left(\frac{D_{SM}}{D_{SE}}\right)^2\left(\frac{D_{MV}}{384,400km}\right)^2 \qquad \text{(V)}$$

This is our initial estimate of the effective lunar reflectance and it is this that is used in all future lunar calibrations as the reflectance standard. Corrections to this lunar reflectance for phase angle and libration come from scaling the effective disk reflectance model to be consistent with the initial APS observations. The model for the effective disk reflectance is given by [Kieffer and Stone 2005]

$$\begin{aligned}\ln A_k^{USGS}(g,\Phi,\theta,\phi) = \sum_{i=0}^{3} a_{ik}g^i + \sum_{j=0}^{3} a_{jk}\Phi^{2j-1} + c_1\theta + c_2\phi + c_3\Phi\phi + \\ d_{1k}e^{-g/p_1} + d_2ke^{-g/p_2} + d_{3k}\cos[(g-p_3)/p_4)]\end{aligned} \qquad \text{(W)}$$

where g is the absolute phase angle (in deg), θ and ϕ are the selenographic latitude and longitude of the observer (in deg), and Φ is the selenographic longitude of the sun (in deg). Since the illuminated fraction of the moon is a function of the phase angle, disk-equivalent reflectances for the USGS model of a partially illuminated moon are incorporated into the phase dependent term. The fractional illumination of the moon is also included in the model of Helfenstein and Veverka [1987].

The predicted effective disk reflectance for a lunar calibration characterized by the celestial geometry (g_i, θ_i, ϕ_i, Φ_i) can then be tied to the effective disk reflectance observed by the APS sensor immediately after its solar calibration, with celestial geometry (g_0, θ_0, ϕ_0, Φ_0), by the expression

$$A_k = A_k^{APS}\,\frac{A_k^{USGS}(g_i,\Phi_i,\theta_i,\phi_i)}{A_k^{USGS}(g_0,\Phi_0,\theta_0,\phi_0)} \qquad \text{(X)}$$

which means that the expressions for the radiometric calibration coefficients based on lunar calibration are

$$C0 = \frac{A_k^{APS}\times\frac{A_k^{USGS}(g_i,\Phi_i,\theta_i,\phi_i)}{A_k^{USGS}(g_0,\Phi_0,\theta_0,\phi_0)}\times\frac{F_{0,k}}{\pi\sum_{i,j}\Sigma 1_k(i,j)}}{\frac{\Delta_x\Delta_y}{\Omega_M}\times\left(\frac{D_{SM}}{1AU}\right)^2\left(\frac{D_{MV}}{384,400km}\right)^2} \qquad \text{(Y)}$$

and

$$C0\times C12 = \frac{A_k^{APS}\times\frac{A_k^{USGS}(g_i,\Phi_i,\theta_i,\phi_i)}{A_k^{USGS}(g_0,\Phi_0,\theta_0,\phi_0)}\times\frac{F_{0,k}}{\pi\sum_{i,j}\Sigma 2_k(i,j)}}{\frac{\Delta_x\Delta_y}{\Omega_M}\times\left(\frac{D_{SM}}{1AU}\right)^2\left(\frac{D_{MV}}{384,400km}\right)^2}. \qquad \text{(Z)}$$

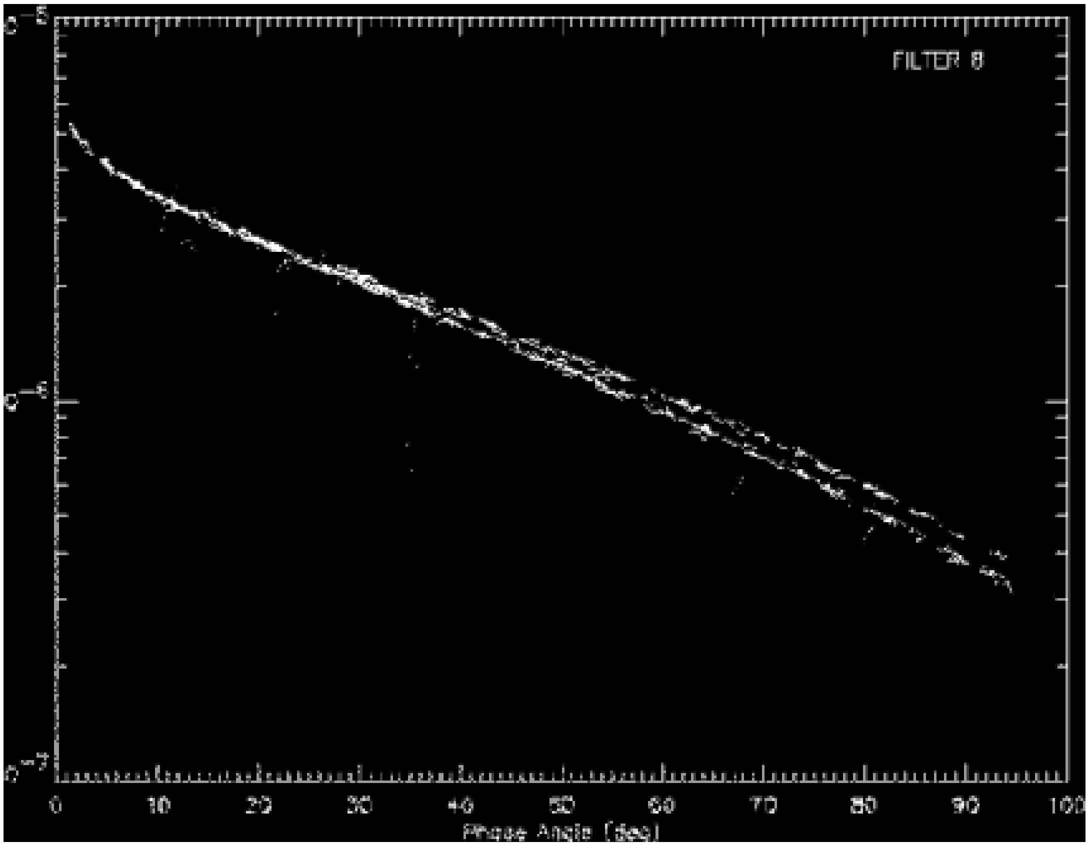

Figure 3.6.2.3-1. Lunar irradiance as a function of phase angle. (Courtesy of ROLO Project.)

4. POLARIMETRIC CALIBRATION

In this section we describe how the polarimetric calibration coefficients that are generated on orbit are calculated and used in the calibration process.

4.1. Unpolarized Reference Calibration

The unpolarized reference provides a source of essentially zero polarization to the APS telescopes by scrambling the polarization of the input scene. The maximum allowed magnitude of the polarized input can be predicted based on the scene data since the mirror used to relay the earth scene through the unpolarized reference is designed such that the unpolarized reference scenes come from the nadir direction. Since the scrambler provides a minimum polarization suppression of 100, scenes over thick clouds where the polarization is low (<10%), and the scene is bright, will provide input polarizations to the APS telescopes of less than 0.1%. A sample of unpolarized reference data taken over relatively thin clouds near Monterey is shown in Figure 4.

The observations of the unpolarized reference can be modeled as

$$C0 \times (R1L - D1Lm) = \frac{I\left(1 + \alpha_q \tilde{q}_{inst}\right)}{2} \qquad \text{(A)}$$

$$C0.K1(R1R - D1Rm) = \frac{I\left(1-\alpha_q \tilde{q}_{inst}\right)}{2} \tag{B}$$

$$C0.C12 \times (R2L - D2Lm) = \frac{I\left(1+\alpha_u \tilde{u}_{inst}\right)}{2} \tag{C}$$

$$C0.C12.K2(R2R - D2Rm) = \frac{I\left(1-\alpha_u \tilde{u}_{inst}\right)}{2} \tag{D}$$

where the m suffix to the RXY measurements indicates an average over the valid sectors that view the unpolarized reference and the other constants and calibration coefficients have been defined in the previous sections. Although the coefficients α_q and α_u are also calibration coefficients, any errors in their definition, based on the previous calibration, will have a very small effect (of order 10^{-8}, based on errors in instrumental polarization being stable at the 0.05% level and orbit-to-orbit variations in the α coefficients being less than 0.01%). Their values are therefore assumed to be given by the previous calibration.

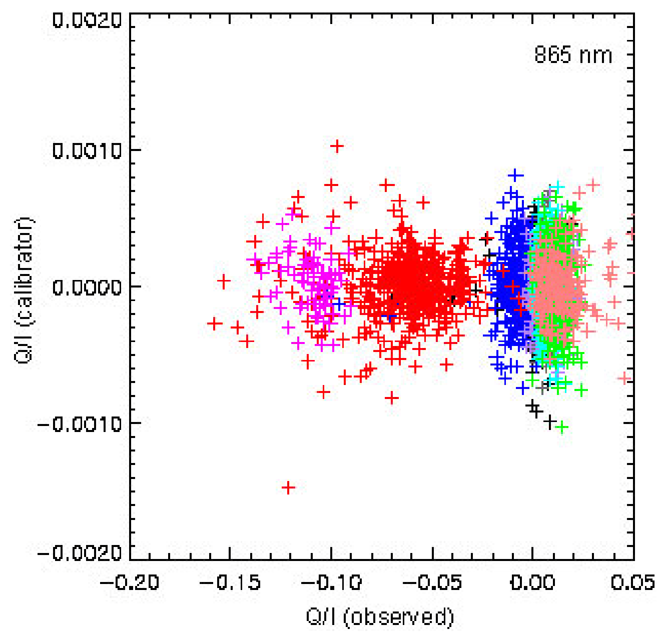

Figure 4.1-1. Single shot discrepancies between the ground-based calibration with input polarizations less than 0.01% and the unpolarized reference implemented for the RSP instrument. The cloud optical depth was typically around ten and this figure therefore represents a conservative expectation of how well the un-polarized reference will work, even at the single shot level, over cloud decks.

We now construct calibration expressions for the K1 and K2 coefficients viz.,

$$K1 = \frac{\left(1-\alpha_q \tilde{q}_{inst}\right)}{\left(1+\alpha_q \tilde{q}_{inst}\right)} \frac{(R1Lm - D1Lm)}{(R1Rm - D1Rm)} \tag{E}$$

$$K2 = \frac{\left(1-\alpha_u \tilde{u}_{inst}\right)}{\left(1+\alpha_u \tilde{u}_{inst}\right)} \frac{(R2Lm - D2Lm)}{(R2Rm - D2Rm)}. \tag{F}$$

These coefficients can and will be calculated for each scan of data, but it is expected that the update of the K1 and K2 coefficients will only occur on an orbit-by-orbit time scale since the typical variation of these coefficients for an aircraft instrument of similar design is less than 0.1% over the course of a year of sporadic aircraft operations.

4.2. Polarized Reference Calibration

The polarized reference provides a highly polarized input to the APS sensor with a well-defined azimuth. The relationship of the APS observations of the polarized reference to the α coefficients can be modeled as

$$\alpha_q \approx \frac{\{-\cos(2\varepsilon_1)q_{cal} - \sin(2\varepsilon_1)u_{cal}\} + \tilde{q}_{inst}}{\delta 1m \times \xi(p_{cal})} \qquad \text{(G)}$$

and

$$\alpha_u \approx \frac{\{\sin(2\varepsilon_2)q_{cal} - \cos(2\varepsilon_2)u_{cal}\} + \tilde{u}_{inst}}{\delta 2m \times \xi(p_{cal})} \qquad \text{(H)}$$

where the various parameters except q_{cal} and u_{cal} have been defined above. q_{cal} and u_{cal} are the normalized Stokes parameters of the polarized reference in the absolute reference frame of the APS measurements. Since the expected polarization from the calibration reference in the reference frame of the Wollaston prisms is easily derived (cf. equation 20 in section 2) a more useful operational definition of the expression for the calibration coefficients is

$$\alpha_q \approx \frac{\tilde{q}_{cal} + \tilde{q}_{inst}}{\delta 1m \times \xi(p_{cal})} \qquad \text{(I)}$$

and

$$\alpha_u \approx \frac{u_{cal} + \tilde{u}_{inst}}{\delta 2m \times \xi(p_{cal})} \qquad \text{(J)}$$

where the notation for the calibration coefficients follows from equation (20) of section 2.

5. REFERENCES

R. A. Barnes et al., 2003: Comparison of the on-orbit response history of SeaWiFS with the USGS lunar model, *Appl. Opt*.

Robert A. Barnes, Robert E. Eplee, Jr., Frederick S. Patt, 1998: SeaWiFS measurements of the moon, *Proc. SPIE* **3438**, 311-324.

B. Cairns, L.D. Travis and E.E. Russell, Research Scanning Polarimeter: Calibration and ground-based measurements, *Proc. SPIE*, **3754**, 186-197, Denver 1999.

P. Helfenstein, and J. Veverka, 1987: Photometric properties of lunar terrains derived from

Hapke's equations, *Icarus*, **72**, 342-357.

H. H. Kieffer, and T. C. Stone, 2005: The spectral irradiance of the Moon, Ap. J., 128, 2887-2901.

H. H. Kieffer, and J. M. Anderson, 1998: Use of the Moon for spacecraft calibration over 350-2500 nm, in *Sensors, Systems, and Next Generation Satellites II*, H. Fujisada, ed, *Proc. SPIE* **3498**, 325-336.

Slater, P.N., S.F. Biggar, K.J. Thome, D.I. Gellman, P.R. Spyak, "Vicarious radiometric calibrations of EOS sensors", *J. Atmos. Ocean. Technol.*, **13**, 349-359 (1996).

T.C. Stone, H. H. Kieffer, and K. J. Becker, "Modeling the radiance of the Moon for on-orbit calibration," in *Earth Observing Systems VIII*, W. L. Barnes, ed., *Proc. SPIE* **5151**, 463-470 (2003).

C. Wehrli, "Spectral solar irradiance data," World Climate Research Program (WRCP) Publication Series No. 7, WMO ITD No. 149 (World Meteorological Organization, Geneva, Switzerland, 1986) pp. 119-126.

Robert H. Woodward et al., "Modeling of the SeaWiFS Solar and Lunar Observations," *NASA Technical Memorandum 104566*, Vol. 10, May 1993.

Project ROLO, (1 July 2002), http://www.moon-cal.org/.

A. STATIC AND INITIAL CALIBRATION COEFFICIENTS

Polarimetric

Wollaston Prisms

	410	443	555	670	865	910	1378	1610	2250
Absolute Orientation ('	44.933	44.627	44.881	44.622	44.861	44.626	44.729	44.721	44.728
Relative Orientation (°	0.2046	-0.447	0.1902	-0.419	0.1788	-0.416	0.1766	0.1764	0.1767

Polarimetric Scale Factor

Reciprocal of aq	0.9857	0.9796	0.9962	0.9965	0.9980	0.9984	0.9936	0.9957	0.9939
Reciprocal of au	0.9857	0.9786	0.9973	0.9965	0.9992	0.9993	0.9940	0.9964	0.9948

Relative Gain Factors

K1	1.0041	0.9823	1.0115	1.0187	0.9900	0.9910	1.0104	1.0098	0.9907
K2	0.9929	0.9793	1.0134	0.9917	0.9953	0.9967	1.0054	1.0258	1.0050

Only the 410 nm band needs to be corrected for instrumental polarization and this correction depends on viewing direction.

Instrumental Polarization

Angle/Calibrator	PRA	50.2	36.1	23.9	22.5	12.2	0	-12.2	-22.5	-23.9	-36.1	-47.8	-62.3	URA
Earth View Sector	3,4	8	38	64	67	89	115	141	163	166	192	217	248	7,8
q_inst	0.0006	0.0025	0.0022	0.0018	0.0018	0.0013	0.0008	0.0000	0.0000	0.0000	0.0003	0.0008	0.0018	0.0031
u_inst	0.0003	-0.0001	-0.0002	0.0000	0.0000	0.0002	0.0002	0.0002	-0.0002	-0.0002	-0.0008	-0.0012	-0.0018	-0.0018

Radiometric

Calibration Coefficients Units are W/m2/um/sr/DN

Noise Model is of the form Noise=sqrt(floor + shot*intensity_in_DN) and is in units of DN.

	410	443	555	670	865	910	1378	1610	2250
C0	0.0053	0.0059	0.0056	0.0053	0.0034	0.0028	0.0007	0.0006	0.0002
C0_Redundant	0.0053	0.0059	0.0056	0.0053	0.0034	0.0028	0.0007	0.0006	0.0002
ARA1	0.0285	0.0277	0.0269	0.0257	0.0261	0.0254	0.0590	0.0469	0.0477
RSA1	0.0150	0.0150	0.0150	0.0150	0.0150	0.0151	0.0181	0.0159	0.0154
DN1@Lmax	51465.4	50302.9	52159.5	50837.6	51628.2	51103.4	51146.8	51799.4	50727.2
Headroom1	0.2267	0.2551	0.2104	0.2419	0.2229	0.2354	0.2344	0.2188	0.2446
SNR1@Ltyp	926.8	748.0	811.5	575.4	522.2	423.4	219.3	609.0	397.8
Floor1	42.2990	41.0747	16.2897	13.5077	8.6873	20.5268	10.2917	7.0373	12.3837
Shot1	0.0049	0.0049	0.0031	0.0028	0.0026	0.0042	0.0233	0.0033	0.0052
Tintx1.2	1.2040	1.2036	1.2036	1.2034	1.2031	1.2027	1.2041	1.2031	1.2033
Tintx0.8	0.7957	0.7961	0.7963	0.7963	0.7967	0.7969	0.7998	0.7971	0.7969
Cal2	0.0053	0.0058	0.0057	0.0054	0.0034	0.0028	0.0007	0.0006	0.0002
Cal2_Red	0.0053	0.0058	0.0057	0.0054	0.0034	0.0028	0.0007	0.0006	0.0002
ARA2	0.0285	0.0276	0.0269	0.0256	0.0259	0.0254	0.0588	0.0470	0.0476
RSA2	0.0150	0.0150	0.0150	0.0150	0.0150	0.0151	0.0181	0.0159	0.0154
DN2@Lmax	51049.2	51175.0	51647.1	50336.4	50517.1	51256.4	48491.4	52844.6	50755.1
Headroom2	0.2367	0.2337	0.2224	0.2543	0.2498	0.2317	0.3020	0.1947	0.2439
SNR2@Ltyp	923.3	768.3	795.7	569.8	510.6	424.8	216.9	611.7	401.1
Floor2	41.0197	41.1242	16.9029	13.5337	8.7036	20.7027	15.2806	7.0491	14.0111
Shot2	0.0049	0.0046	0.0032	0.0029	0.0027	0.0042	0.0220	0.0034	0.0050
Tintx1.2	1.2038	1.2038	1.2035	1.2035	1.2030	1.2027	1.2041	1.2029	1.2032
Tintx0.8	0.7958	0.7958	0.7964	0.7962	0.7968	0.7968	0.7999	0.7973	0.7970
C12	1.0082	0.9830	1.0099	1.0100	1.0220	0.9970	1.0548	0.9802	0.9995
C12_Redundant	1.0082	0.9830	1.0098	1.0099	1.0220	0.9970	1.0562	0.9805	0.9993

B. APS Spectral Characterization Summary

Table B-1. APS spectral response integrated against solar spectrum, summary of results. The columns correspond to the solar irradiance at the top of the atmosphere (F0), the spectral locations of the upper and lower points at which the response has 1 % of its peak value (FW1Pl and FW1Ph), the spectral locations of the upper and lower points at which the response has 50% of its peak value (FWHMl and FWHMh) and the full width at which the responses is at 50% of its maximum value.

F0	FW1P (lo)	FWHM (lo)	Center	FWHM (hi)	FW1P (hi)	FWHM
W/m2/µm	nm	nm	nm	nm	nm	nm
1732.8	396.737	403.775	413.273	422.232	430.507	18.4574
1899.39	426.54	433.571	443.586	452.55	459.438	18.9783
1842.84	539.918	545.293	555.235	565.314	572.08	20.0212
1505.83	658.116	663.664	673.873	684.64	692.234	20.9751
960.464	829.103	845.52	865.747	886.033	901.653	40.5122
895.586	886.924	901.361	910.626	920.476	929.956	19.1151
354.553	1347.71	1356.44	1375.51	1392.67	1405.5	36.2277
245.697	1551.52	1577	1603.31	1629.46	1651.7	52.4507
73.3686	2193.39	2220.46	2260.39	2299.68	2327.78	79.2183

Table B-1

C. Absolute Orientation of APS Views with respect to the nominal nadir point

Scene Type	Behavior	Relative to scan start		Relative to nadir		Relative to nadir		Number of samples
		Time at start	Time at end	Time at start	Time at end	Angle start	Angle end	
Dark Reference	DC Restore	0	9	-336	-327	-157.5	- 153.28125	10
Dark Reference	Sampling	10	25	-326	-311	-152.8125	- 145.78125	16
Polarized Reference	Sampling	125	131	-211	-205	-98.90625	-96.09375	7
Earth	Sampling	221	475	-115	139	-53.90625	65.15625	255
Unpolarized Reference	Sampling	513	523	177	187	82.96875	87.65625	11
Solar Reference	Sampling	618	634	282	298	132.1875	139.6875	17
Dark Reference	Sampling	743	758	407	422	190.78125	197.8125	16
Dark Reference	DC Restore	759						Indefinite (Resync)

D. SIS Radiance Levels used during APS testing

Units are W/m2/um/sr

	lvl27	lvl26	lvl25	lvl24	lvl23	lvl22	lvl21	lvl20	lvl19	lvl18	lvl17	lvl16	lvl15	lvl14
(nm)	ABCDEFGI	ABCDEFIJ	ABCDEFG	BCK	ABC	GH	BDF	B	DE	DG	AFDI(55	AFI (55%	AFI (70%	AD
412	339.48	261.49	200.26	150.68	114.24	77.99	61.85	49.73	44.23	40.17	30.34	26.150	25.487	21.919
443	544.13	419.37	321.95	239.16	183.22	124.76	99.38	79.34	70.64	64.63	49.91	43.039	41.933	35.733
555	1473.16	1134.96	879.88	635.73	499.00	338.20	270.99	211.80	191.43	178.46	145.65	125.807	122.495	102.663
672	2344.93	1808.05	1410.47	996.44	796.38	536.89	432.32	332.05	304.64	287.54	244.09	210.743	205.062	170.627
865	2728.74	2092.48	1698.69	1167.90	952.17	636.25	516.43	388.94	363.61	346.96	306.29	263.978	256.531	211.532
910	2724.02	2106.11	1663.21	1141.14	935.17	617.90	507.59	381.44	356.58	338.64	303.76	261.866	254.048	209.785
1378	1169.34	902.98	717.71	490.01	400.91	266.36	223.31	165.45	152.93	147.89	138.98	119.745	115.236	95.186
1610	832.22	646.09	509.59	343.42	282.85	186.13	157.27	116.40	107.81	103.80	98.82	85.135	81.877	67.586
2250	201.76	156.96	123.98	83.45	68.79	45.20	37.61	28.24	25.88	24.96	23.17	20.088	19.332	16.439

	lvl13	lvl12	lvl11	lvl10	lvl9	lvl8	lvl7	lvl6	lvl5	lvl4	lvl3	lvl2	lvl1	
	AI (55%)	A	DFI	DFI (55%	F	DI (25%	DI (55%	D	I	I @ 25%	I @ 35%	I @ 55%C	I @ 70%	Closed
412	18.216	17.276	15.287	13.068	7.934	6.828	5.135	4.194	3.159	2.634	2.174	0.940	0.277	
443	29.875	28.303	25.270	21.610	13.163	11.254	8.447	6.875	5.231	4.379	3.619	1.572	0.466	
555	86.458	81.733	74.703	63.912	39.349	32.897	24.563	19.839	15.516	13.058	10.829	4.725	1.413	
672	143.822	135.705	126.588	108.381	66.921	55.579	41.461	33.343	26.324	22.235	18.487	8.117	2.437	
865	178.800	168.151	161.495	138.144	85.178	71.123	52.966	42.316	34.001	28.807	24.004	10.650	3.203	
910	177.609	166.547	161.796	137.217	84.257	71.885	52.960	41.899	35.640	29.986	25.123	11.061	3.243	
1378	81.133	74.765	77.596	64.219	38.612	35.903	25.607	19.239	19.745	16.664	13.878	6.368	1.858	
1610	57.947	53.220	55.291	45.599	27.189	25.755	18.411	13.684	14.418	12.070	10.178	4.726	1.468	
2250	13.836	12.831	12.761	10.341	6.271	5.944	4.070	3.062	3.417	2.865	2.497	1.025	0.238	

E. Solar Reference Assembly Geometrical Details and Spectralon BRDF

Spacecraft coordinate system

This coordinate system is the one that is fixed relative to the orientation of the APS spacecraft hardware. In this coordinate system the solar vector changes with orbital motion and the solar diffuser surface normal vector remains fixed. The +z axis is nominally in the nadir direction of the APS optical system. The +x direction is parallel to the velocity vector of the spacecraft. The +y direction is orthogonal to both as defined by the right-hand rule. The Scan Mirror Assembly rotates the APS detector field-of-view in a scan plane that is parallel with the spacecraft x-z plane.

Unit vector coordinates at the center of the SRA diffuser surface

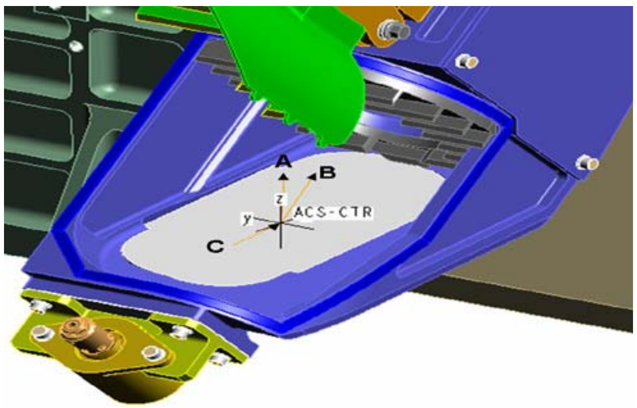

Figure E1. Solar diffuser panel surface and telescope optical axis vectors

The following diagram show the solar diffuser as housed in the Solar Reference Assembly. The origin of a Cartesian coordinate axis is placed at the center of the diffuser so as to define the spacecraft coordinate system at that location.

Three vectors, A B and C, are shown that are related to the orientation of the solar diffuser surface. These are defined as:

A. The diffuser surface normal vector.

B. The vector representing the optical axis of the Polarimeter Module telescopes/Scan Mirror Assembly when the system is aligned with the center of the solar diffuser. This vector was the original design center of the APS and is retained here for consistency with Raytheon documentation.

C. The vector representing the orientation of the major axis of the diffuser surface in the spacecraft coordinate system. Note that it is slightly offset from the line resulting from the intersection of the plane of the diffuser surface with the Scan Mirror Assembly (SMA) scan plane so it is not quite parallel to the x-z plane of the spacecraft coordinate system. The vector, as shown, is pointing in the direction the optical axis of the APS telescopes would move across the surface of the diffuser as the San Mirror Assembly rotates.

Table E-1. Summary of orientations of the APS view of the solar reference assembly (SRA) diffuser, the solar view of the diffuser and the available unvignetted range of the solar reference assembly. NB: The SRA samples in this table are zero based such that the 17 samples are indexed 0 to 16. For the unvignetted SRA calculations of SMA angle relative to nadir 6 milliradians of margin was included to account for 4 milliradians of drag smear (integration time) and the 8 milliradian IFOV. The unvignetted SMA range based on the mechanical design is provided for information as the last line in this table.

	Vector A	**Vector B**	**Vector C**	**Unvignetted SRA**		**Solar (Nominal)**
SRA Sample				10	11	
Dist from Nadir				292	293	
x	-0.121587	0.692409	0.992581	0.683592302	0.677598305	-0.915803
y	-0.155269	0	-0.019065	0	0	-0.047995
z	0.980361	0.721505	0.120082	0.729864073	0.735432211	0.398749
SMA Angle(°)		136.1788762		136.5312253	137.6875247	
AOI/AOV		51.45365743		50.77152674	50.31235352	59.84985591
Unvignetted Range		136.156	137.844			

Table E-1

Spectralon Bidirectionl Reflectance Distribution Function (BRDF) characterization

The measurements of the Spectralon™ witness samples were made at NASA Goddard Space Flight Center. Measurements of direct hemispherical reflectance were made at Labsphere. The BRDF measurements do not cover the full spectral range of the APS and the Labsphere DHR measurements are therefore needed to provide a scaling of the measured BRDF at shorter wavelengths to those needed at longer wavelengths.

Two types of measurements were therefore made at GSFC. One set of measurements had an angle of incidence of 8° and view angles every 7.5° from 0° to 82.5° at azimuths of 0°, 90° and 180°. These measurements were integrated to get an 8° illumination DHR that is comparable to that provided by Labsphere. The azimuthally averaged BRDF measurements from GSFC are given in Table E-2. Note the BRDF of an ideal Lambertian surface is $1/\pi$.

Table E-2. Azimuthally averaged BRDF values with illumination at 8°.

View Angle °	Wavelength (nm)							
	325	457	488	514	633	670	780	835
0	0.3373	0.3427	0.3437	0.3430	0.3440	0.3443	0.3457	0.3473
7.5	0.3360	0.3418	0.3420	0.3415	0.3420	0.3423	0.3433	0.3455
15	0.3340	0.3400	0.3400	0.3397	0.3400	0.3400	0.3407	0.3427
22.5	0.3310	0.3357	0.3363	0.3353	0.3360	0.3360	0.3367	0.3383
30	0.3277	0.3323	0.3327	0.3317	0.3330	0.3327	0.3330	0.3350
37.5	0.3240	0.3287	0.3290	0.3283	0.3290	0.3290	0.3293	0.3307
45	0.3197	0.3243	0.3250	0.3240	0.3247	0.3243	0.3247	0.3257
52.5	0.3150	0.3193	0.3193	0.3193	0.3187	0.3183	0.3187	0.3203
60	0.3080	0.3127	0.3127	0.3120	0.3117	0.3120	0.3127	0.3127
67.5	0.2997	0.3030	0.3033	0.3033	0.3033	0.3030	0.3033	0.3040
75	0.2867	0.2910	0.2910	0.2903	0.2897	0.2900	0.2907	0.2910
82.5	0.2663	0.2693	0.2693	0.2677	0.2673	0.2673	0.2673	0.2677

Table E-2

The comparison of Labsphere and GSFC measurements of DHR with 8° illumination is given in Table E-3. The GSFC azimuthally averaged BRDF values were integrated over view angle using interpolation to Gaussian quadrature points. Ten, twenty and forty quadrature points were used no apparent difference in the integrated DHR. Note that although a BRDF can have values greater than 1/π the DHR determines the total flux reflected by an object and is therefore necessarily less than unity. This comparison suggests that the BRDF measured at GSFC is 2±0.25 % too bright.

	GSFC	Labsphere	Flight Sample	Ratio
Wavelength (nm)	DHR(8°)	DHR(8°)	Variability	GSFC/Labsphere
325	0.992	0.968	0.64%	1.024
457	1.006	0.987	0.23%	1.019

488	1.007	0.988	0.17%	1.019
514	1.005	0.988	0.15%	1.017
633	1.005	0.988	0.06%	1.018
670	1.005	0.988	0.06%	1.018
780	1.007	0.987	0.10%	1.020
835	1.010	0.987	0.06%	1.023

Table E-3. DHR with 8° illumination angle.

The BRDF for the relevant flight geometry made use of the reciprocity between illumination and viewing directions in order to simplify the measurement process. The angle of view of the SRA is always 50.5°±0.25°. Since it is easier experimentally to move the detector than the source, BRDF measurements were made with a fixed angle of incidence of 50° and viewing angles varying from 55° to 65° over an azimuth range of 0° to 10° (i.e. we interchanged the geometries of source and detector). In Table E4 we show the average and standard deviation over wavelength of the BRDF when multiplied by π and divided by the GSFC DHR at 8°. It can be seen that over the spectral range of 400 to 850 nm variation from the mean in the BRDF is typically 0.4% or less. We therefore use this generic BRDF, scaled by the Labsphere measurements of the DHR at 8° illumination of the flight unit witness samples, to generate the reflectances needed in the use of the SRA.

Table E-4. Spectrally averaged values of π BRDF(λ)/DHR(λ l,8°) for the reciprocal of the APS SRA observational viewing geometry.

	Relative Solar Azimuth ($\Delta\phi$°)									
	180		177.5		175		172.5		170	
AOI °	Mean	Std	Mean	Std	Mean	Std	Mean	Std	Mean	Std
55	1.1814	0.3%	1.1822	0.3%	1.1796	0.4%	1.1769	0.4%	1.1729	0.4%
57.5	1.1898	0.4%	1.1903	0.4%	1.1894	0.4%	1.1876	0.3%	1.1849	0.5%
60	1.1979	0.4%	1.1983	0.4%	1.1996	0.4%	1.1965	0.4%	1.1952	0.4%
62.5	1.2068	0.4%	1.2081	0.4%	1.2086	0.4%	1.2072	0.5%	1.2054	0.5%
65	1.2161	0.4%	1.2170	0.4%	1.2184	0.4%	1.2179	0.4%	1.2166	0.4%

Table E-4

Operationally this means that the reflectance required for solar calibration is determined by interpolating, within the set of values provided within this table (Table E-4), to the solar illumination and viewing geometry for the current APS scan. That value is then multiplied by the appropriately solar spectrally weighted Labsphere DHR values for the APS bands that are given in Table E-5.

Table E-5. APS 8° illumination DHR values calculated from Labsphere measurements of the APS flight unit witness pieces.

Table E-5

Band	Center (nm)	DHR@8°	Std Dev
1	413.3	0.9866	0.24%
2	443.6	0.9864	0.22%
3	555.2	0.9881	0.11%
4	673.9	0.9877	0.10%
5	865.7	0.9877	0.09%
6	910.6	0.9876	0.12%
7	1375.5	0.9835	0.07%
8	1603.3	0.9837	0.08%
9	2260.4	0.9563	0.36%

In order to calculate the orientation of the view and illumination vectors with respect to the SRA Spectralon reflector it is helpful to supplement the vectors A and C introduced above with their cross-product and define a unit vector system in the frame of the Spectralon diffuser. In this frame **z**' is the normal to the Spectralon, **x**' is the direction of the orientation of the major axis of the diffuser surface and **y**' is the orientation of the minor axis of the diffuser surface. The formulae for obtaining the azimuth (ϕ_S) and zenith (θ_S) of the sun relative to the Spectralon™ diffuse reflector using the solar vector (**s**) in the spacecraft co-ordinate system from the APS ACS packet are

$$\begin{aligned}&\cos\theta_S = \mathbf{s.z'} \Rightarrow \theta_S = \arccos(\mathbf{s.z'})\\ &\left.\begin{aligned}\sin\theta_S\cos\phi_S &= \mathbf{s.y'}\\ \sin\theta_S\sin\phi_S &= \mathbf{s.x'}\end{aligned}\right\} \Rightarrow \phi_S = \arctan(\mathbf{s.x'}/\mathbf{s.y'})\end{aligned} \qquad \text{B1}$$

The supplementary co-ordinate system of the diffuser is defined with respect to the spacecraft co-ordinate system in Table E-6.

Table E-6. Co-ordinate system for the normal to the Spectralon (z') and the vectors that define the plane of the Spectralon surface (x' and y') expressed in the spacecraft co-ordinate system so that the formulae in Eq. B1 can be computed.

	z'	x'	y'
x	-0.121587	0.992581	4.55704E-05
y	-0.155269	-0.019065	0.987688112
z	0.980361	0.120082	0.156435115

Table E-6

The same formulae apply to determining the azimuth (ϕ_v) and zenith (θ_v) of the view incidence vector **v** relative to the Spectralon. The view incidence vector is dependent on the sector of data that is being used and can be determined for each of the seventeen sectors associated with observations of the SRA using the expressions

$$\begin{aligned} v_x &= \sin(2\pi((282 + sra\_index)/768)) \\ v_y &= 0 \\ v_z &= \cos(2\pi(0.5 - (282 + sra\_index)/768)) \end{aligned} , \qquad \text{B2}$$

where *sra_index* is zero based (running from 0 to 16 for the 17 available sectors). As noted above, the only sectors for which unvignetted data are expected are sectors 10 and 11. Given the slow variation of BRDF with view the GSFC measured geometry with an AOV (illumination zenith) of 50° is used for all calibrations even though the actual AOV is either 50.8°, OR 50.3°. Based on the variation of BRDF with angle this assumption may introduce a bias of 0.2% into the solar calibration. The azimuth of the view incidence vector changes even less with *sra_index* and so for the expected calibration sectors for APS a view azimuth of 81.5±0.1° is used. The solar azimuth can therefore be calculated relative to this value and the relative azimuth which is needed to get the correct reflectance value in Table E-4 is $\Delta\phi$=81.5-ϕ_s.

For reference Table E-7 provides a set of sample solar vectors from the Glory mission simulation during the solar calibration maneuver together with the Spectralon illumination zenith and relative (to 81.5°) solar illumination azimuth calculated using Eq. B-1.

Table E-7. Example of calculating required AOI and relative azimuth of solar and view directions from solar vector in spacecraft co-ordinate system that is reported in APS ACS packet. Note that the AOI of the sun on the Spectralon is less than 65° with valid spacecraft azimuth 3±3° for 80 seconds during the solar calibration maneuver. At the end of this set of ACS data the spacecraft is in the center of the target box and it is therefore expected that valid solar calibration data would be obtained for 160 seconds.

t (secs)	835774893	835774903	835774913	835774923	835774933	835774943	835774953	835774963	835774973
x	-0.94974	-0.946535	-0.943213	-0.939833	-0.936324	-0.932772	-0.929078	-0.925281	-0.921397
y	-0.053346	-0.054185	-0.055038	-0.055986	-0.056895	-0.057672	-0.05872	-0.059643	-0.060682
z	0.308461	0.318018	0.327598	0.337015	0.346497	0.355822	0.365193	0.374563	0.383856
x'	0.426162	0.435272	0.444392	0.453361	0.462371	0.471202	0.480102	0.488970	0.497769
y'	-0.904636	-0.900291	-0.895827	-0.891324	-0.886685	-0.882024	-0.877213	-0.872301	-0.867310
z'	-0.004478	-0.003812	-0.003156	-0.002619	-0.002033	-0.001341	-0.000910	-0.000356	0.000072
θ	64.775754	64.197394	63.615526	63.040490	62.459790	61.887674	61.307924	60.727108	60.147467
ϕ	89.716362	89.757411	89.798178	89.831675	89.868639	89.912864	89.940538	89.976614	-89.995265
ϕ corrected	-90.283638	-90.242589	-90.201822	-90.168325	-90.131361	-90.087136	-90.059462	-90.023386	-89.995265
$\Delta\phi$	171.783638	171.742589	171.701822	171.668325	171.631361	171.587136	171.559462	171.523386	171.495265
S/C Azimuth	3.057952	3.106093	3.155039	3.209440	3.261605	3.306197	3.366345	3.419321	3.478960

Table E-7

The correction to ϕ is included to emphasize that a two argument (e.g. atan2) inverse tangent should be used otherwise the quadrant that the inverse tangent lies in must be identified explicitly and used to correct the standard arctangent call.

F. Calibration of a telescope with a channel missing

In the event that one a pair of channels in a telescope becomes inoperable it will be necessary to modify the calibration method applied to the remaining good channel. The following approach assumes that the same band in the other telescope is still functioning normally. Simplifying the equations in the body of this document for the purposes of defining the calibrations approach for a single channel we find that:

$$C0.S1L = \frac{I + q_{inst}Q + u_{inst}U + \frac{1}{\alpha_q}[q_{inst}I - Q]}{2} \tag{F1a}$$

$$C0.K1.S1R = \frac{I + q_{inst}Q + u_{inst}U - \frac{1}{\alpha_q}[q_{inst}I - Q]}{2} \tag{F1b}$$

$$C0.C12.S2L = \frac{I + q_{inst}Q + u_{inst}U + \frac{1}{\alpha_u}[u_{inst}I - U]}{2} \tag{F1c}$$

$$C0.C12.K2.S2R = \frac{I + q_{inst}Q + u_{inst}U - \frac{1}{\alpha_u}[u_{inst}I - U]}{2} \tag{F1d}$$

We will define an additional calibration coefficient CX which applies to any "oddball" channels since these channels cannot be calibrated in the normal manner. This nomenclature is acceptable since there can only be one "oddball" per band. Let us now examine what is observed when looking through the unpolarized reference assembly.

$$CX.S1L = \frac{I\left(1 + \frac{q_{inst}}{\alpha_q}\right)}{2} \tag{F2a}$$

$$CX.S1R = \frac{I\left(1 - \frac{q_{inst}}{\alpha_q}\right)}{2} \tag{F2b}$$

$$CX.S2L = \frac{I\left(1 + \frac{u_{inst}}{\alpha_u}\right)}{2} \tag{F2c}$$

$$CX.S2R = \frac{I\left(1 - \frac{u_{inst}}{\alpha_u}\right)}{2} \tag{F2d}$$

The intensity through the URA is determined from the telescope that has both channels for this band (i.e. if Telescope 1 has a missing channel then I_2 is used and if Telescope 2 has a missing channel then I_1 is used). The formulae for determining CX for an "oddball" channel are as follows:

$$CX. = \frac{I_2\left(1 + \frac{q_{inst}}{\alpha_q}\right)}{2S1L} \tag{F3a}$$

$$CX = \frac{I_2\left(1 - \frac{q_{inst}}{\alpha_q}\right)}{2.S1R} \tag{F3b}$$

$$CX = \frac{I_1\left(1 + \frac{u_{inst}}{\alpha_u}\right)}{2.S2L} \tag{F3c}$$

$$CX = \frac{I_1\left(1 - \frac{u_{inst}}{\alpha_u}\right)}{2.S2R} \tag{F3d}$$

The "oddball" channels are polarimetrically calibrated using views through the PRA, for which the observations are modeled as,

$$\alpha_q = \frac{(q_{inst} - q_{cal})}{\left(\frac{2.CX.S1L}{I_2} - 1\right)} \tag{F4a}$$

$$\alpha_q = \frac{(q_{inst} - q_{cal})}{\left(\frac{2.CX.S1R}{I_2} - 1\right)} \tag{F4b}$$

$$\alpha_u = \frac{(u_{inst} - u_{cal})}{\left(\frac{2.CX.S2L}{I_1} - 1\right)} \tag{F4c}$$

$$\alpha_u = \frac{(u_{inst} - u_{cal})}{\left(\frac{2.CX.S2R}{I_1} - 1\right)} \quad \text{(F4d)}$$

where terms of the form $p_{inst}.p_{cal}.cos(\chi_{inst}-\chi_{cal})$ are neglected since they are small compared with the other uncertainties in this calibration method. The other uncertainties are related to small differences in the intensities that can be observed in different telescopes as a result of slightly different boresight alignment, or transmission differences of the mirrors and/or windows. The definition of aq and aq for these "oddball" channels is slightly different from normal, depending on the channel, but this difference (sign change) is only used to compensate for sign changes in the calculation of q and u in the next step.

The final quantity that is required from the "oddball" channel calibration is q, or u depending on which telescope is suffering from a lost channel.

$$q = q_{inst} - \alpha_q\left(\frac{2.CX.S1L}{I_2} - 1\right) \quad \text{(F5a)}$$

$$q = q_{inst} - \alpha_q\left(\frac{2.CX.S1R}{I_2} - 1\right) \quad \text{(F5b)}$$

$$u = u_{inst} - \alpha_u\left(\frac{2.CX.S2L}{I_1} - 1\right) \quad \text{(F5c)}$$

$$u = u_{inst} - \alpha_u\left(\frac{2.CX.S2R}{I_1} - 1\right) \quad \text{(F5d)}$$

In fact throughout this analysis it is not necessary to use I_1, or I_2 since all quantities are ratios. Instead S1L+K1*S1R and S2L+K2S2R can be used instead as long as the usage is consistent.